NASA Technical Memorandum 83411

Low Flight Speed Acoustic Results for a Supersonic Inlet With Auxiliary Inlet Doors

Richard P. Woodward, Frederick W. Glaser,
and James G. Lucas
Lewis Research Center
Cleveland, Ohio

Prepared for the
Nineteenth Joint Propulsion Conference
cosponsored by the AIAA, SAE, and ASME
Seattle, Washington, June 27-29, 1983

NASA

LOW FLIGHT SPEED ACOUSTIC RESULTS FOR A SUPERSONIC INLET WITH AUXILIARY INLET DOORS

Richard P. Woodward, Frederick W. Glaser, and James C. Lucas
National Aeronautics and Space Administration
Lewis Research Center
Cleveland, Ohio

Abstract

A model supersonic inlet with auxiliary inlet doors and boundary layer bleeds was acoustically tested in simulated low speed flight up to Mach 0.2 in the NASA Lewis 9x15 Anechoic Wind Tunnel and statically in the NASA Lewis Anechoic Chamber. A JT8D refan model was used as the noise source. Data were also taken for a CTOL inlet and for an annular inlet with simulated centerbody support struts. Inlet operation with open auxiliary doors increased the blade passage tone by about 10 dB relative to the closed door configuration although noise radiation was primarily through the main inlet rather than the doors. Numerous strong spikes in the noise spectra were associated with the bleed system, and were strongly affected by the centerbody location. The supersonic inlet appeared to suppress multiple pure tone (MPT) generation at the fan source. Inlet length and the presence of support struts were shown not to cause this MPT suppression.

E-1694

Introduction

There is concern about the fan noise radiated from supersonic inlets, particularly during takeoff and, possibly, approach, which are the two flight conditions when the community surrounding the airport is most adversely affected by excessive noise. This noise will also be affected by the required variable geometry of the inlet assembly. These assemblies may require auxiliary inlet flow area in the form of doors or annular slots. Little is known about the effects of these auxiliary doors on either the generation of fan noise or its propagation. In addition, these inlets employ a variable inlet area mechanism, such as a translating centerbody, to adjust inflow conditions. Centerbody and cowl bleeds are features that are primarily included to help control shock generated boundary layer separation at supersonic cruise conditions. Thus, the supersonic inlet assembly has several geometric features which could complicate forward-radiated noise.

References 1 and 2 present static aeroacoustic results for a supersonic inlet with auxiliary doors, bleeds, and translating centerbody. The test vehicle was a YF-12 aircraft operated statically. Results showed that all of the variable geometry components affected noise generation.

The present study is an effort to define the aeroacoustic properties of a supersonic inlet operating in two controlled test environments. The test inlet, designated the "P-inlet,"[3,4] was tested in simulated low speed flight up to Mach 0.2 in the NASA Lewis anechoic wind tunnel,[5,6] and statically in the NASA Lewis anechoic chamber.[7] Acoustic results are presented for far-field microphones as well as for internal pressure sensors located on the inlet duct walls. Corresponding aerodynamic results for the anechoic tunnel tests are presented in Ref. 8. Baseline acoustic data for a conventional flight-contoured inlet (CTOL inlet) on the JT8D refan are included for comparison. The acoustic effect of long support struts was investigated using an annular inlet with simulated struts which approximated those found in the P-inlet. This inlet was also tested with the struts removed.

Apparatus

Anechoic Tunnel Installation

Figure 1 shows a cross-sectional view of the P-inlet as it was tested in the Lewis anechoic wind tunnel. A JT8D refan model[9] was mated to the inlet as shown in Fig. 1 for this test series. This fan, which has inlet guide vanes and operates at high tip speed, was selected as having characteristics representative of the fan noise expected from future supersonic transport engines. Design parameters for the JT8D refan model are given in Table I. Results presented for the anechoic wind tunnel installation are for a 0.2 tunnel Mach number except where otherwise noted. The inlet in the tunnel had sharp lips at the highlight and door openings typical of a flight configuration.

Auxiliary inlet doors are required on a supersonic inlet to allow sufficient airflow to reach the fan during takeoff conditions, where relatively low forward flight speed and high airflow requirements prevail. A primary purpose of this investigation was to assess the acoustic impact of opening these auxiliary doors with their additional noise path and circumferential flow distortion. The P-inlet was run with 40%, 20% and closed door configurations as shown in Fig. 1. The percent door opening was calculated as the ratio of the door throat area to the disk area projected by the inlet cowl lip. The closed door configuration was achieved by covering only the door outer surface. Each of the four doors extended circumferentially over a 50° arc. Four axially aligned centerbody support struts (L/H = 4) were located midway between the doors in the horizontal and vertical directions.

The P-inlet assembly cowl and centerbody walls have porous surfaces in the throat region consisting of many small holes (1.6 mm diam) which, in flight, remove wall boundary layers and exhaust the low velocity air to the atmosphere. This inlet bleed system is intended to prevent terminal shock boundary layer separation at design speeds and to provide some margin of inlet subcritical operating stability.[10,11] The cowl and centerbody bleed holes were always open to the internal airflow. The closed bleed tests were performed by taping the bleed exit louvers on the outside of the inlet. The centerbody bleed had a complicated path (see Fig. 1) connecting the outside bleed louvers to the centerbody orifices through the hollow support struts and the fixed centerbody cylinder.[3] The cylinder connects to selected cavities behind bleed holes in the concentric translating centerbody depending on

centerbody position. At high flight speeds the lower pressure at the external bleed exits compared to the internal pressures results in positive bleed flow from inside to outside. However, reverse bleed flow did occur under static conditions and at the 0.2 Mach number simulated flight speed of the tunnel. The actual magnitude of the bleed flow was not measured in the current tests.

The JT8D refan model was driven by a multi-stage air turbine in the tunnel installation. The turbine exhaust exited on the inside of the translating cone which acted as the fan stage plug nozzle. This arrangement tended to shield the microphones from the turbine noise. The aerodynamic survey rakes[8] (Fig. 1) were found not to affect the acoustic results, and thus were left installed for all tests.

Figure 2 is a photograph showing the P-inlet installed in the anechoic wind tunnel. Part of the far field (1.83 M radius) microphone array is visible in this photograph. The plan view of this tunnel installation is shown in Fig. 3. The auxiliary door and cowl lip microphones were mounted on the inlet assembly about 2.5 cm from the surface. All microphones were 0.64 cm diameter, oriented to point upstream, and equipped with aerodynamic nose cones with side openings to minimize airflow-induced noise. In addition to the microphones, there were a number of dynamic pressure transducers located in the flow passages to allow diagnostic study of the internal noise field. Acoustic calibration of the anechoic wind tunnel has shown the test section to be anechoic at frequencies above 1000 Hz.[6]

Anechoic Chamber Installation

The P-inlet assembly with the JT8D refan model was also tested in the Lewis anechoic chamber. The inlet and auxiliary doors had bellmouth lips to better simulate flight airflow for these static tests (Fig. 4). In addition, an inflow control device (ICD) was attached to the inlet to help establish flight-quality airflow into the inlet.[12] It was not possible to similarly treat the airflow entering the auxiliary doors.

The JT8D refan model was remotely driven by an electric motor in the anechoic chamber installation. The fan airflow exited into an exhaust collector and out of the facility. Figure 5 is a photograph showing the P-inlet installation in the anechoic chamber. The ICD has been removed for this photograph. Figure 6 shows a similar view of the P-inlet with the ICD installed.

Figure 7 shows a plan view of the P-inlet installation in the anechoic chamber. Far field (0.64 cm diam) microphones were located in 10° increments from 0° to 90° from the inlet axis. There were no microphones located adjacent to the inlet assembly; however, the same internal pressure transducers were used in the chamber installation as in the tunnel installation. Only the forward-radiated noise (including door-radiated noise) was measured in the chamber, unlike the tunnel where there was a possibility for aft-radiated noise contamination. Acoustic calibration of the anechoic chamber has shown it to be anechoic at frequencies above 200 Hz.

The JT8D refan was also tested in the anechoic chamber with a CTOL inlet for baseline noise comparisons with the P-inlet. As shown in Fig. 8, the same ICD was installed on the CTOL inlet as was used for the P-inlet chamber installation. The far-field microphone array was adjusted to keep the same radius centered on the inlet plane for the shorter CTOL inlet. The CTOL inlet installation had limited internal pressure transducers for diagnostic purposes.

Acoustic Data Reduction

The acoustic data were recorded on magnetic tapes for later 50 Hz constant bandwidth spectral analysis. The output of this narrow-bandwidth sound pressure level (SPL) analysis was digitized and transmitted to a computer for further analysis. Using a computer data reduction program, narrow-bandwidth sound power level (PWL) spectra were generated for the forward quadrant (0 to 90 degrees from the fan inlet axis) for the chamber results.

Results and Discussion

Aerodynamic Results

Detailed aerodynamic results for the P-inlet test are reported in Ref. 8. The fan operating map for the JT8D refan model is shown in Fig. 9 (see Table I for fan stage design parameters). This performance was typical of the fan in all installations. Data were taken for fan operation from 50 to 90 percent of design speed.

Acoustic Results

The acoustic results are presented in two groups. The first group is for lower fan speeds where the spectra are characterized by tones at the blade passing frequency and its harmonics, while the second group is for higher fan speeds where shaft order tones dominate the noise spectra.

Flight Effect

Figure 10 shows the effect of simulated flight in the anechoic wind tunnel. The SPL spectra are for the fan operating at 60% design speed, which, for this inlet configuration (fully extended centerbody, 40% open auxiliary doors, and closed bleeds), gives an inlet throat Mach number of about 0.38. The data are for the microphone at 70° from the inlet axis. These spectra show a reduced "skirting" of the blade passage tone (BPF) with increasing tunnel flow, indicating improved airflow at the sharp inlet lip. The actual level of the BPF tone shows little change with flight showing that internal noise mechanisms, such as inlet guide vane-rotor interaction, control the tone level. The absence of higher tone harmonics (2 x BPF and 3 x BPF) when there is no tunnel flow remains unexplained. The spectrum for the fan at windmill (about 15% design fan speed) with the tunnel at 0.2 Mach number shows that the tunnel background noise level has no effect on the test results above 1000 Hz.

Test Facility Effects

Figure 11 shows a spectral comparison for the P-inlet in the two test facilities. For reference a spectrum of the refan noise with the CTOL inlet is also shown. The SPL spectra are at 70° from the inlet axis with the fan operating at 60% design speed. The anechoic chamber data are adjusted to the 1.83 M radius of the tunnel microphone. The P-inlet was operated with 40% open auxiliary doors and closed bleeds. The P-inlet centerbody spike was extended 50% in the tunnel, while in the cham-

ber it was extended 40%. The P-inlet throat Mach numbers were about 0.42 in both installations, while with the CTOL inlet the throat Mach number was slightly lower.

The fundamental tone levels (BPF) for the P-inlet are about the same in both installations, indicating that these tones are controlled by sources other than installation effects. Likewise, there is good agreement for the P-inlet overtone levels. The strong tones between the fundamental and first overtone are resonant tones which seem to be associated with the inlet bleed systems. These tones, which appear to be quite sensitive to inlet configuration and centerbody position, will be discussed in detail in a later section of this report. The P-inlet results for the tunnel installation typically showed a higher level in the 1 to 4 kHz range than did the corresponding chamber results. The reason for this difference is unknown, but seems to relate to the tunnel airflow.

With the CTOL inlet there was good agreement in broadband noise with the P-inlet results. However, the fundamental tone and the second overtone (3 x BPF) for the CTOL inlet are considerably higher than the corresponding P-inlet results. Earlier investigators (see Ref. 1) have shown that the installation of a supersonic inlet may reduce the fan noise levels relative to those for a CTOL inlet. However, in Ref. 1, the fan was operating in the supersonic tip speed range, rather than subsonically as for Fig. 11, and the entire spectral noise level, rather than just the fundamental tone and its harmonics, was reduced with installation of the supersonic inlet.

nlet Mach Number Effect

The sound attenuation effects of near-sonic flow at an inlet throat have been reported in the literature.[13] This effect in the P-inlet results from the anechoic chamber is shown in Fig. 12, where the overall sound power level (OAPWL, 1 to 20 kHz) is plotted as a function of inlet throat Mach number. The inlet bleeds are closed. The variation in mass averaged inlet throat Mach number for a particular auxiliary door configuration was achieved by axially translating the inlet centerbody. The attenuation produced by increasing Mach number is evident at about 0.7 throat Mach number. There is a considerable noise attenuation toward Mach unity for the closed auxiliary doors configuration, showing sonic inlet behavior. The lesser attenuation for the open door configurations with increasing Mach number suggests that some noise may be radiating through the auxiliary doors.

The results for the CTOL inlet are similar to the P-inlet results at the subsonic (50% and 60% design) fan speeds. However, the CTOL inlet results are about 6 dB higher than those for the P-inlet at 80% design fan speed where MPT noise can occur. Thus the P-inlet appears to prevent or attenuate the far field radiation of MPT noise in a region of relatively low throat Mach number. Again, the nature of the MPT noise of the refan with the P-inlet will be discussed in more detail in a later section of this report.

Auxiliary Door Effect

For takeoff, and possibly approach, it may be necessary to open the auxiliary doors to provide sufficient fan airflow. With open door operation there is a clear possibility that nonuniform airflow will reach the fan. Also, open doors provide an additional path for acoustic radiation. Finally, opening the doors reduces the inlet throat Mach number. All of these effects could lead to an increase in the radiated noise.

The fundamental tone directivity results of Fig. 13 show a tone level increase at all angles with open auxiliary doors that is typical of this inlet. The cowl and centerbody bleeds were closed for the investigation of the auxiliary door effect. In Fig. 13 the tone level increases almost 10 dB at all forward angles with 40% open doors relative to the results with closed doors. The difference between levels for 40% and 20% open doors becomes less toward the aft angles.

The data for the 90° and 110° aft positions relative to the auxiliary doors (see Fig. 3) show little effect of door opening. This unexpected result suggests that the door-induced noise is primarily radiated through the inlet mouth rather than through the door openings or, if through the doors, is radiated forward.

Narrow bandwidth spectra are presented in Fig. 14 for the 10° and 70° data of Fig. 13. At 10° from the inlet axis (Fig. 14(a)) the fundamental and first overtone are seen to increase with door size. No clear tones were observed for the closed door configurations. Instead the closed-door spectrum shows a "haystack" in the vicinity of the BPF, but at a somewhat lower frequency. Although the reason for this behavior is unknown, it may be associated with the somewhat higher throat Mach number (0.74) of the closed door configuration. Figure 12 shows sonic attenuation beginning at about this throat Mach number.

The 70° results in Fig. 14(b) show a similar weak tone increase as the doors are opened. At this angular location the fundamental tone for the closed door configuration peaks at the same frequency as the fundamental tones for the open door configurations. The lower broadband level for the closed door configuration above 10 kHz is unexplained but may be related to the lower throat Mach number. Several resonance tone spikes are seen in the spectrum of Fig. 14(b).

As an aid to separating source and propagation effects, it is useful to look at the internal pressure spectra. Figure 15 shows spectra corresponding to the conditions of Fig. 14 but measured at a location on the outer flow passage wall between the auxiliary door opening and the refan stage inlet guide vane. Again, there is a tone level increase associated with open door operation. This clearly shows that the tone level increase which was observed in the far field is a source effect associated with the auxiliary door inflow. The broadband level for the closed door configuration in Fig. 15 may relate to the higher throat Mach number and consequent scrubbing noise potential for this configuration. It is also interesting to note that, although haystacked, the fundamental tone for the closed door configuration is centered at the BPF in Fig. 15 in contrast to the corresponding spectrum of Fig. 14(a).

Bleed Effect

Throat region boundary layer bleeds are used to help prevent terminal shock boundary layer separation at design speeds and to increase inlet subcritical operating stability. It is desirable to leave the inlet bleed system open at all times for simplicity of operation. However, little is known of the acoustic effects of the bleed system. The P-inlet had both cowl and centerbody bleed systems

(see Fig. 1) which were ducted to the outer surface of the inlet. The centerbody bleed system was especially complicated. Depending on centerbody position, different translating centerbody cavities were opened to the hollow centerbody. The bleed airflow also travels through passages in the centerbody support struts to external exhaust ports. At high flight Mach numbers the lower pressure at these exit ports compared to the internal pressures would insure positive bleed flow. However, at low forward flight speed (0.2 Mach) and during static operation these bleed systems experienced reverse flow. No measurements of the bleed flow magnitude was made during these tests. The bleeds were closed by taping over the external duct openings leaving some internal bleed cavities open to the internal flow.

Strong resonance tones related to the bleed system geometry were observed in the P-inlet results. As seen in the spectra of Fig. 16, the number, frequency and magnitude of these tones were sensitive to both centerbody location and the bleed system configuration. Curiously, in the far field results, these strong resonance tones were almost entirely restricted to the angles from 50° to 90°. Also, the occurrence of these resonance tones was greatest at the lower fan speeds and for the mid-range centerbody positions. The spectra in Fig. 16 are for the tunnel installation at 50% design fan speed and 70° from the inlet axis. At the 50% centerbody extension (Fig. 16(a)) various resonance tones appear in response to the opening of different bleed ducts. The one exception is that with the centerbody bleed open to flow and the cowl bleed closed there were no observable resonance tones in the spectrum. It should be noted that these resonance tones have no frequency relationship to the rotor interaction tones and their harmonics. Retracting the centerbody to the 25% extended position (Fig. 16(b)) results in an entirely different set of resonance tones being generated. The frequency of these spikes does not correspond to either cavity resonance frequency or the struhal frequency for vortex shedding from the orifices as they are usually calculated; however, predictions are uncertain due to the complexity of the P-inlet bleed system passages. Thus the generating mechanism of the spikes was not identified.

Data from the external microphone at the cowl lip tended to have the same spectral content as did the data for the 70° microphone. Figure 17 shows the cowl lip spectra corresponding to those of Fig. 16(a). The same resonance tones as were seen in Fig. 16(a) are strongly represented in these spectra. The absence of fan tones (1, 2, 3 x BPF) is conspicuous in Figs. 16 and 17.

As was previously mentioned, these resonance tones were largely restricted to the 70° microphone position results. Directivities for three of the typical resonance tones are presented in Fig. 18. While the tone levels clearly peak at 70°, the corresponding broadband level tends to dip at the same angular position. This irregular broadband behavior is not normally observed in fan noise directivity results and remains unexplained.

References 14 and 15 present data for another supersonic inlet which was tested in the Lewis 10x10 supersonic wind tunnel. In this test lower frequency resonance tones were found to be generated by bypass door cavities. Installation of a blade cascade at the entrance to the cavities eliminated these tones. Additionally, the resonance tones were reduced when airflow passed through the cavities. Although a different region of the inlet internal flow path produced resonance in this reference, there is the similarity that cavity flow, such as centerbody bleed flow in the present study, tended to reduce the resonance tone levels.

Combination Auxiliary Door and Bleed Effects

In an earlier section it was shown that opening the auxiliary doors will increase the fan fundamental tone level. The results presented in that section were for both bleeds closed. Figure 19 shows how the SPL spectra at 70° is affected by opening both bleeds. As in the earlier section, the data are for the tunnel installation at 0.2 Mach number, with the fan operating at 60% design speed and 50% centerbody extension. With 20% open auxiliary doors (Fig. 19(a)) there is essentially no BPF tone effect from opening both bleeds. There is, however, the usual bleed-induced change in resonance tone structure.

A different situation is seen for the 40% open auxiliary doors (Fig. 19(b)) in which opening the bleeds causes about a 7 dB increase in the fundamental tone level. There is no change in the first overtone level. Perhaps the bleed flow enhances the flow nonuniformity effects of the 40% open doors with a consequent rise in the fundamental BPF tone level.

The fundamental tone directivities for the operating conditions in Fig. 19 show a similar effect of the bleed flow at other inlet angles. Open bleeds have little effect on the fundamental tone level (except for a single point at 90°, forward arc) with 20% open doors (Fig. 20(a)). With 40% open doors (Fig. 20(b)) opening the bleeds increases the fundamental tone level by 5 to 7 dB in the 30° and 70° range. The bleed effect is slightly reversed at the forward arc 10° and 90° positions. As in Fig. 13, no clear data trends are seen in the aft 90° and 110° results.

Data from the internal pressure transducers can be an effective tool in isolating the fan inlet noise mechanisms. Figure 21 shows internal pressure spectra at a number of locations in the P-inlet for the anechoic tunnel installation. Spectra for the external microphones at the cowl lip and auxiliary door lip are also shown. These data are for the fan operating at 60% design speed, centerbody 50% extended, 40% open auxiliary doors, and both bleeds open. Figure 21 clearly shows the development of the resonance tones. These tones are especially strong along the centerbody and outer cowl just upstream of the bleed openings. The resonance tones become weaker toward the fan stage, and are not at all present just downstream of the fan stage. These data support the idea that the resonance tones originate in the bleed system, and especially in the centerbody bleed system. This idea is reinforced by the observation that the resonance tone structure varies with centerbody position.

The corresponding internal spectra for the anechoic chamber installation of the P-inlet are shown in Fig. 22. These data are for the centerbody 40% extended, so a change in the resonance tone structure is expected. The external lip microphones were not installed in the chamber. Again, in Fig. 22, the resonance tones are strongest in the inlet throat region and especially just upstream of the centerbody bleed.

Multiple Pure Tone Attenuation

An unexpected observation from earlier supersonic inlet tests has been the apparent attenuation

of fan multiple pure tones (MPT's) even though the inlet throat Mach number was too low to expect acoustic choking effects.[1] In the present investigation internal sound measurements show that the P-inlet somehow causes a reduction in the actual MPT generation at the fan source.

Figure 24 shows how the overall sound power level (OAPWL) (1 to 20 kHz, 0° to 90°) varies with fan speed for the refan with the CTOL inlet and with the P-inlet in the anechoic chamber. The P-inlet was run with 40% open auxiliary doors and closed bleeds. The centerbody was 50" extended. Open doors are necessary with P-inlet operation above 70% design fan speed to avoid hard choking at the inlet throat. Above 70% design fan speed, strong MPT generation controls the OAPWL level for the CTOL inlet. The OAPWL for the P-inlet shows a modest increase at 80% speed, then decreases rapidly at higher fan speeds. At 90% design fan speed the P-inlet throat Mach number for this configuration is only 0.68, so, from Fig. 12, acoustic choking effects are unlikely.

Figure 25 compares the PWL spectra at 80% fan speed for the two inlet configurations of Fig. 24. As seen in this figure the MPT content for the P-inlet is much less than for the CTOL inlet where the entire spectrum consists of MPT's. Additionally, the fundamental rotor alone tone, which is clearly evident for the CTOL inlet, is essentially missing in the P-inlet results. At 80% fan speed the MPT content and fundamental rotor alone tone level for the P-inlet increase somewhat with additional centerbody extension. However, at higher fan speeds translating the centerbody has little effect on the MPT's.

Figure 26 compares the SPL spectra at 70° from the inlet axis for the P-inlet in the two facilities at 80% design fan speed. The centerbody is 50% extended in the tunnel; 40% extended in the chamber. The tunnel Mach number is 0.2. In these results the fundamental rotor alone tone level is somewhat higher for the tunnel installation. (At 75% centerbody extension the fundamental tone levels were essentially identical in the two facilities.) A strong resonance tone is seen in the tunnel data. The far field MPT level is similar for the P-inlet in the two facilities since the MPT structure in the chamber seems to fall within the corresponding spectral envelope for the tunnel data.

Internal spectra provide an insight into the MPT generation mechanism. The internal spectra for the CTOL inlet with the refan operating at 80% design speed (Fig. 26) show strong MPT content throughout the inlet. There is even evidence of weak MPT's downstream of the fan.

In contrast, only modest MPT levels are seen in the corresponding internal spectra for the P-inlet in the tunnel installation (Fig. 27) and the chamber installation (Fig. 28). There is, however, excellent agreement between the spectra for the two P-inlet installations.

At 90% design fan speed the blade relative velocity is well into the supersonic range and strong MPT generation is expected. The internal pressure spectra for the refan operating at 90% design speed with the CTOL inlet (Fig. 29) show the expected strong MPT content. The 90% design speed internal spectra data for the P-inlet in the tunnel (Fig. 30) and in the chamber (Fig. 31) show no evidence of MPT content upstream of the fan. Also, the fundamental BPF tone is not evident upstream of the fan in the P-inlet internal data. However, this BPF tone is clearly present internally downstream of the fan in both installations. The BPF tone is also weakly present in the cowl lip microphone spectra of Fig. 30. Although not shown, the BPF tone was also present at all angles in the far field spectra corresponding to Figs. 30 and 31. Thus it is somewhat surprising that the BPF tone would not be detected internally yet be radiated into the far field.

The high broadband level at lower frequencies near the cowl lip location in Fig. 30 are due to sharp lip effects of the tunnel P-inlet configuration at high inlet airflows. The spectra for corresponding locations for the chamber installation (Fig. 31) show a flatter broadband.

It was not possible to operate the P-inlet in the closed-doors configuration above 75% design fan speed without choking the inlet. Figures 32 and 33 show the internal pressure spectra for the CTOL and P-inlets at 75% design fan speed. Again, strong MPT generation is evident in the CTOL inlet results (Fig. 32). As for the higher fan speeds, no MPT content is evident in these P-inlet internal results. At this fan speed with the centerbody fully extended the P-inlet is choked. These P-inlet internal spectra are very similar to those in Fig. 30 for 40% open doors and 90% design speed.

This analysis of the internal spectra for the CTOL and P-inlet clearly shows that the nature of the P-inlet is to suppress the actual generation of MPT's at fan speeds which would otherwise result in strong MPT spectral content. Reference 1 reported a significant MPT and fundamental BPF tone reduction with a YF-12 supersonic inlet, and suggested that the axial centerbody support struts may be responsible for the noise reduction. Tests were conducted with the JT8D refan in the anechoic chamber to investigate possible inlet strut effects on the radiated noise.

For these tests a long annular duct with a bellmouth-like lip was fitted to the JT8D refan (Fig. 34). The inlet had a cylindrical centerbody with a rounded nose. Four equally spaced thin axial struts were located in the annular duct. These struts had L/H ration from 1 to 8, and a "no-strut" case was run by using thin upstream wires to support the centerbody. The inlet lip was fitted with the same inflow control device as was used for the P-inlet tests in the chamber. Figure 35 is a photograph of the long inlet duct configuration in the anechoic chamber. The ICD was removed for this photograph.

Figure 36 shows the effect of fan speed on the overall sound power level (1 to 20 kHz, 0° to 90°) for the baseline CTOL inlet and the long annular inlet. The long inlet results shown are for the struts removed and for a strut L/H = 4, which was the case for the P-inlet support struts. The results for the long inlet show essentially no acoustic effect due to the struts. There are, however, some apparent differences between the two inlets due to duct length.

The far field spectra at 70° from the fan inlet axis also show that the long struts have negligible acoustic effect. At 80% of design fan speed the spectra for the struts removed (Fig. 37(a)) and for struts with L/H = 4 (Fig. 37(b)) are similar, with strong MPT content in both spectra. Thus, the presence of the struts in the P-inlet is apparently not the reason for the observed attenuation. Other effects such as inlet length, radial velocity profile, and throat contraction must be considered in this attenuation mechanism.

Figure 38 shows the effect of all three inlet configurations at 60% design fan speed, where the fan spectra are characterized by prominent fan

fundamental and overtones, with no MPT's. The tone levels at 70° from the fan inlet axis are highest with the CTOL inlet. With the long strut inlet the fundamental tone is only slightly reduced, although the overtones show greater reductions. It is interesting to note that the tone levels are slightly higher with the L/H = 4 struts than with the struts removed - presumably a strut-rotor interaction effect. With the P-inlet (tunnel data) the fundamental tone level is greatly reduced relative to the levels for the other inlets, and the overtones are not detectable in the spectrum. Thus, the observed rotor tone reduction for the P-inlet is not associated with the inlet struts, and is only partially related to inlet length. The total reason for the observed rotor tone and MPT reduction for the P-inlet remains unexplained.

Summary of Results

A supersonic inlet, designated the P-inlet, was tested at a 0.2 Mach forward flight speed in the Lewis 9x15 anechoic tunnel and statically in the Lewis anechoic chamber using a JT8D refan model as the fan source. Internal and far field acoustic data were taken. Baseline data using the refan with a conventional CTOL inlet were also taken in the anechoic chamber. This test program was conducted to investigate the acoustic impact of opening auxiliary inlet doors which are required on a supersonic inlet to provide additional fan airflow at low flight speeds. The acoustic effect of opening internal boundary layer bleed systems, required for more stable internal airflow, and the effect of struts was also investigated.

Significant results of this investigation are as follows:

1. At subsonic fan tip speeds P-inlet operation with open auxiliary doors results in a significant increase in the fan fundamental tone SPL. Internal pressure spectra show that this tone increase occurs at the fan source and is most likely due to changes in fan inflow uniformity caused by the open doors. There is no clear indication that the open doors present a significant additional acoustic radiation pathway. However, corresponding fundamental tone levels for a CTOL inlet were greater than those for any P-inlet configuration.

2. The P-inlet appears to greatly suppress fan multiple pure tone generation at the fan source. Tests with a long annular inlet with axial struts showed that the inlet support struts, of themselves, are not the sound suppression mechanism. The reason for this suppression remains unexplained.

3. Numerous strong tones in the spectra were associated with the bleed system. These tones were not fan-related, and were strongly affected by the centerbody location. The far field directivity of these tones is highly directional, with a peak at about 70° from the inlet axis. Internal SPL spectra suggest that the centerbody bleed system is primarily responsible for these tones.

4. Operation with open bleeds has no effect on the fan fundamental tone level for the closed and 20% open auxiliary door configurations. However, the tone was significantly increased with open bleeds for the 40% open auxiliary door configuration.

References

1. Bangert, L. H., Burcham, Jr., F. W., and Mackall, K. G., "YF-12 Inlet Suppression of Compressor Noise: First Results," AIAA Paper 80-0099, Jan. 1980.
2. Bangert, L. H., Feltz, E. P., Godby, L. A., and Miller, L. D., "Aerodynamic and Acoustic Behavior of a YF-12 Inlet at Static Conditions," NASA CR-163106, Jan. 1981.
3. Boeing Commercial Airlane Company, "Supersonic Test of a Mixed-Compression Axisymmetric Inlet at Angles of Incidence," NASA CR-165686, April 1981.
4. Sorensen, Norman E., and Benczo, Daniel P., "Possibilities for Improved Supersonic Inlet Performance," AIAA Paper 73-1271.
5. Yuska, J. A., Diedrich, J. H., and Clough, N., "Lewis 9-by-15-foot V/STOL Wind Tunnel," NASA TM X-02395, 1971.
6. Rentz, P. E., "Softwall Acoustical Characteristics and Measurement Capabilities of the NASA Lewis 9x15 Foot Low Speed Wind Tunnel," Bolt, Beranek and Newman, Inc., Canoga Park, CA, BBN-3175, June 1976 (NASA CR-135026).
7. Wazyniak, J. A., Shaw, L. M., and Essary, J. D., "Characteristics of an Anechoic Chamber for Fan Noise Testing," NASA TM X-73555, 1977.
8. Wasserbauer, J. F., Cubbison, R. W., and Trefny, C. J., "Low Speed Performance of a Supersonic Axisymmetric Mixed Compression Inlet with Auxiliary Inlets," AIAA Paper 83-1414, June 1983.
9. Moore, Royce D., Kovich, George; Tysl, Edward R., "Aerodynamic Performance of a 0.4066-Scale Model of JT8D Refan Stage," NASA TM X-3356, 1975.
10. Sanders, Bobby W., and Cubbison, Robert W., "Effect of Blade-System Back Pressure and Porous Area on the Performance of an Axisymmetric Mixed-Compression Inlet at Mach 2.50," NASA TM X-1710, 1968.
11. Sanders, Bobby W., and Mitchell, Glenn A., "Increasing the Stable Operating Range of a Mach 2.5 Inlet," AIAA Paper 70-686, June 1970.
12. Feiler, C. E., and Groeneweg, J. F., "Summary of Forward Velocity Effects on Fan Noise," AIAA Paper 77-1319, Oct. 1977 (also NASA TM-73722).
13. "Aircraft Engine Noise Reduction," Conference Proceedings from Lewis Research Center, Cleveland, Ohio, May 16-17, 1972, NASA SP-311, pp. 305-317.
14. Coltrin, Robert E., and Calogeras, James E., "Supersonic Wind Tunnel Investigation of Inlet-Engine Compatibility," AIAA Paper 69-487, June 1969.
15. "Aircraft Propulsion," Conference Proceedings from Lewis Research Center, Cleveland, Ohio, November 18-19, 1970, NASA SP-259, pp. 283-312.

TABLE I. - JT8D REFAN STAGE DESIGN PARAMETERS

Inlet guide vanes	23
Rotor blades	34
Bypass stator vanes	84
Core stator vanes	56
Rotor tip diameter, cm (in.)	50.8 (20)
Rotor tip speed, m/sec (ft/sec)	488 (1600)
Inlet weight flow, kg/sec (lbm/sec)	35 (77)
Bypass ratio	2.032
Bypass stage total pressure ratio	1.67

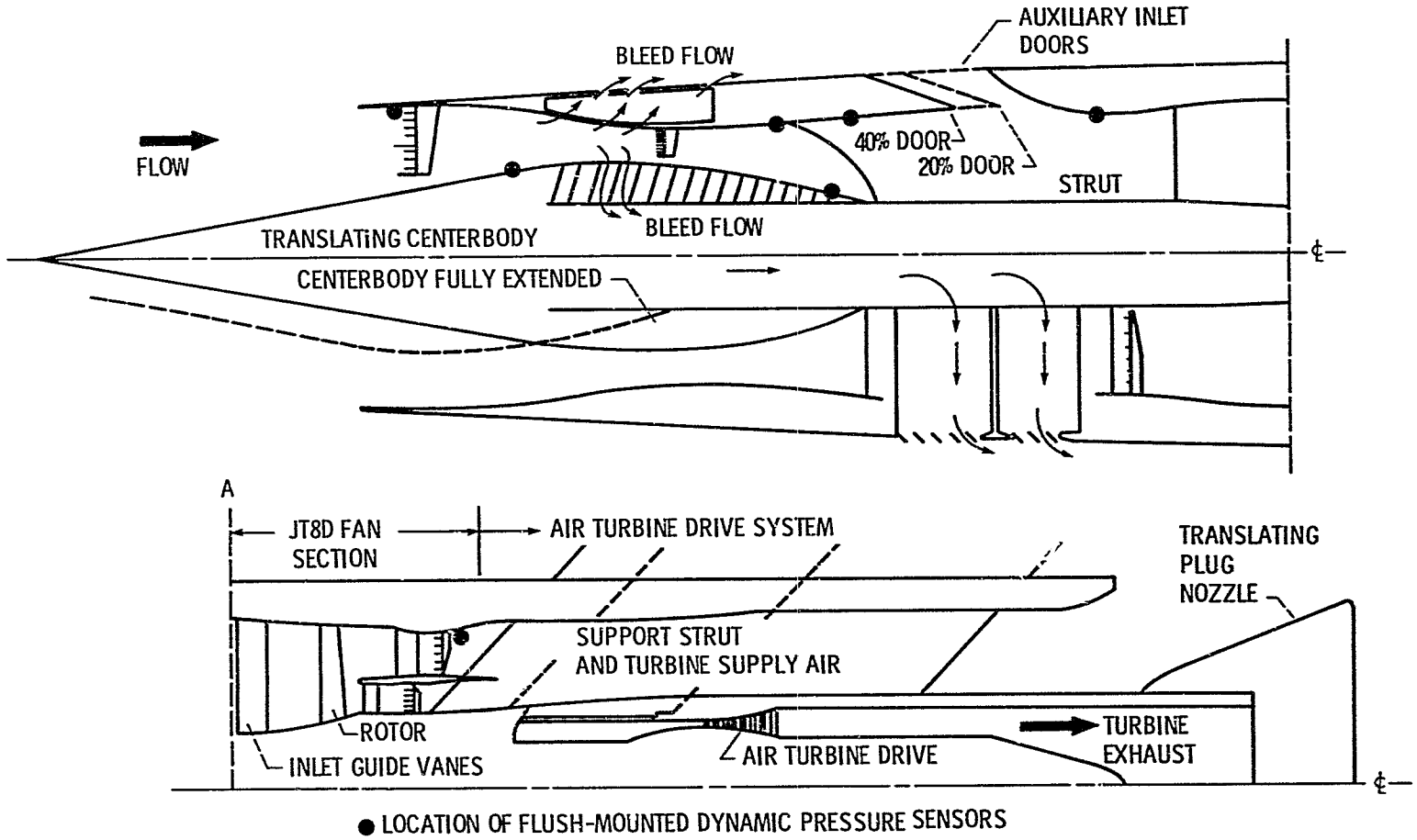

Figure 1. - Cross-sectional view of p-inlet assembly as tested in the 9x15 anechoic wind tunnel. (Shown with centerbody fully retracted).

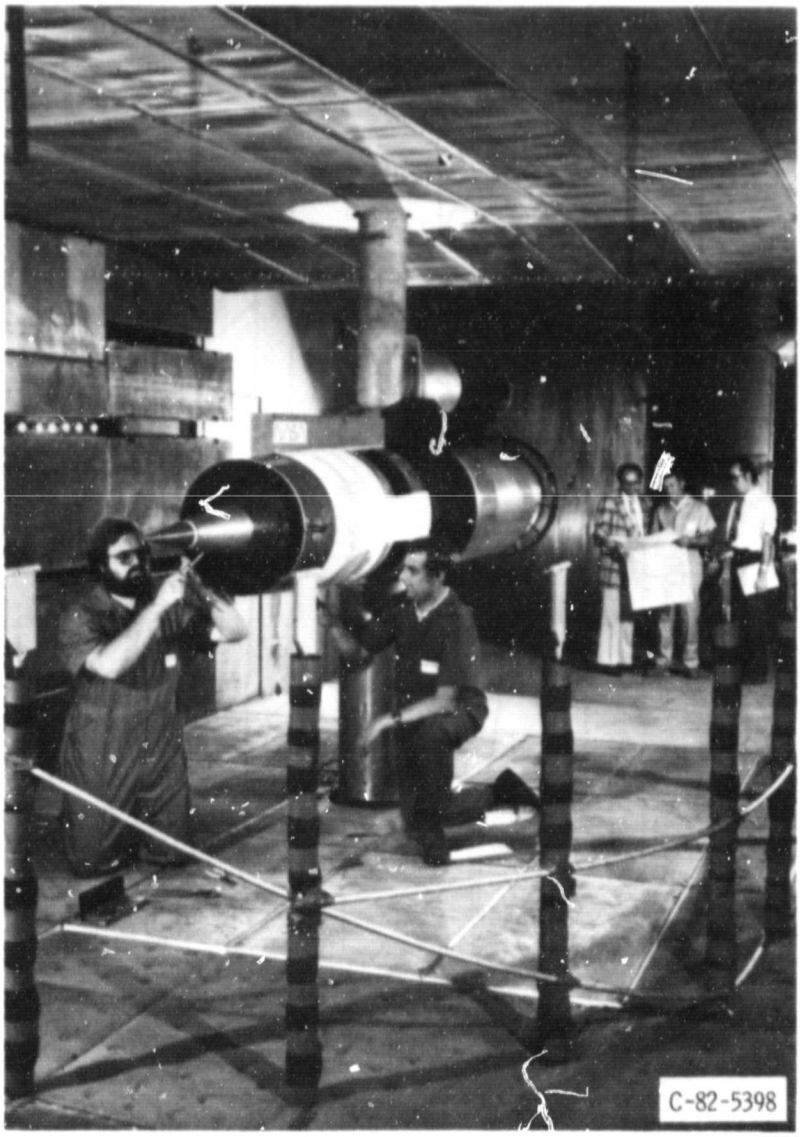

Figure 2. - P-inlet installed in Lewis 9x15 Anechoic Wind Tunnel.

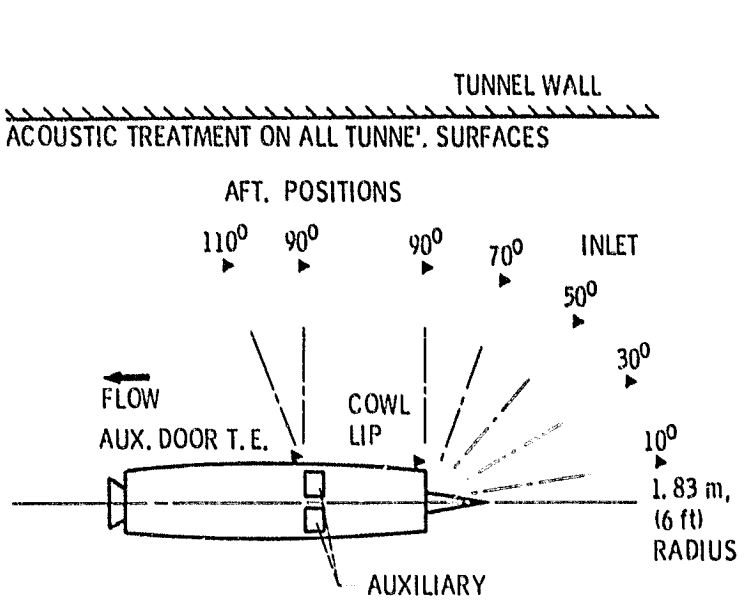

Figure 3. - Plan view of anechoic tunnel test section.

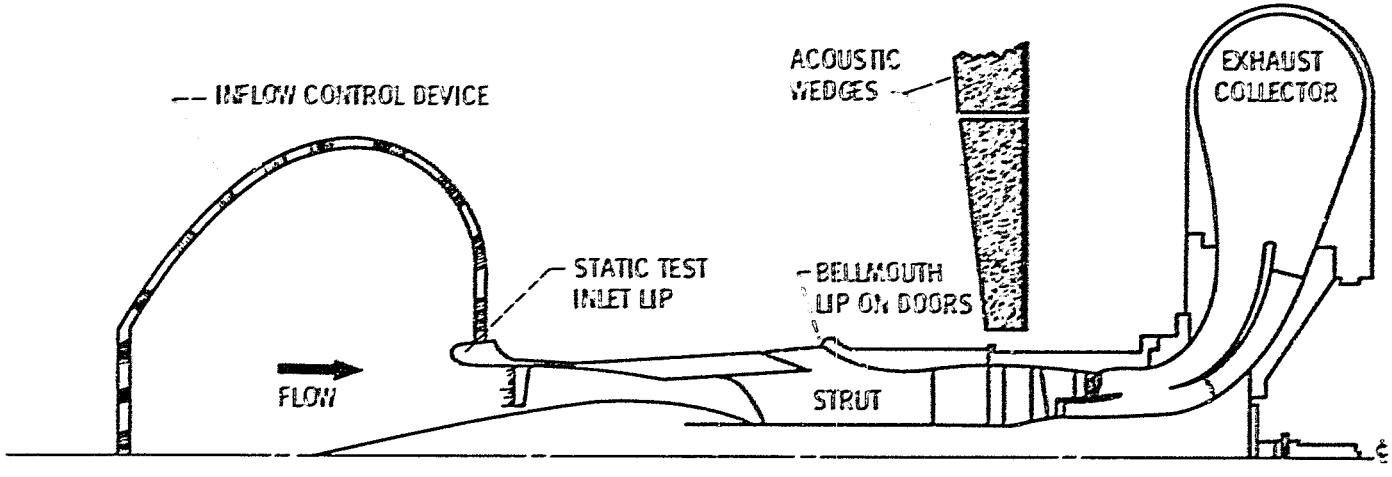

Figure 4 - Cross sectional view of p-inlet assembly as tested in the anechoic chamber.

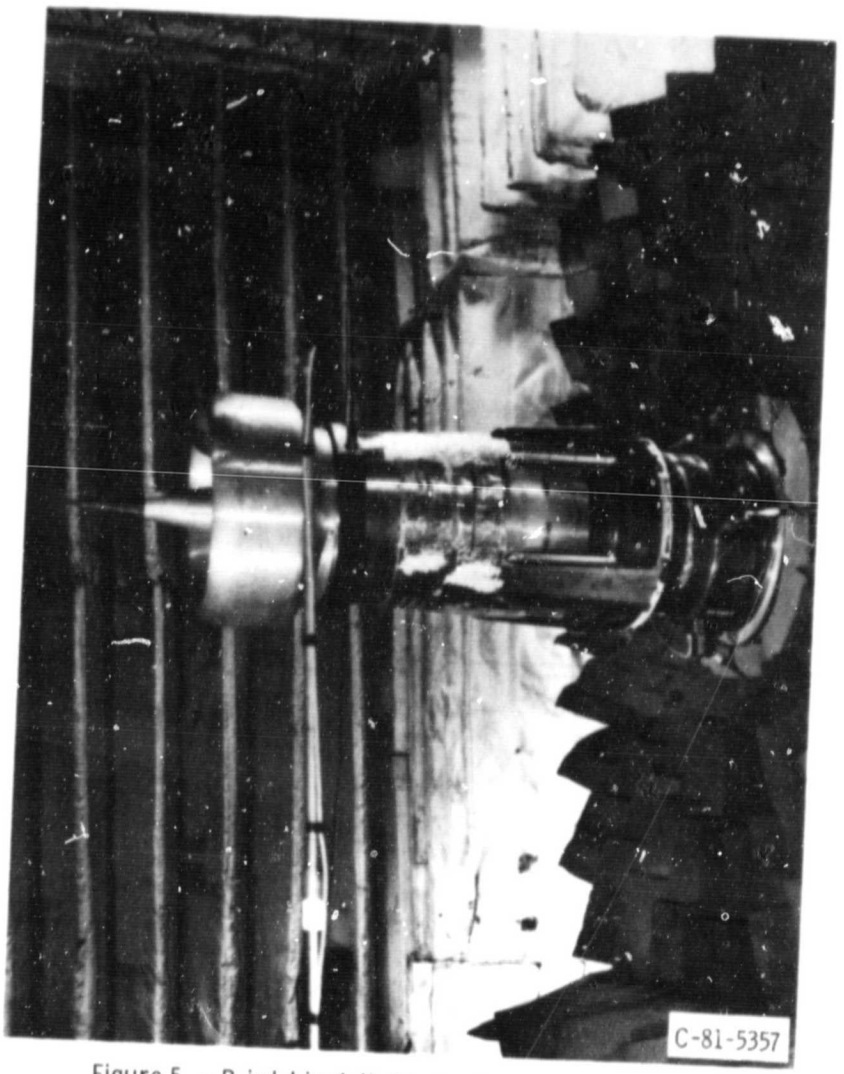

Figure 5. - P-inlet installed in Lewis Anechoic Chamber

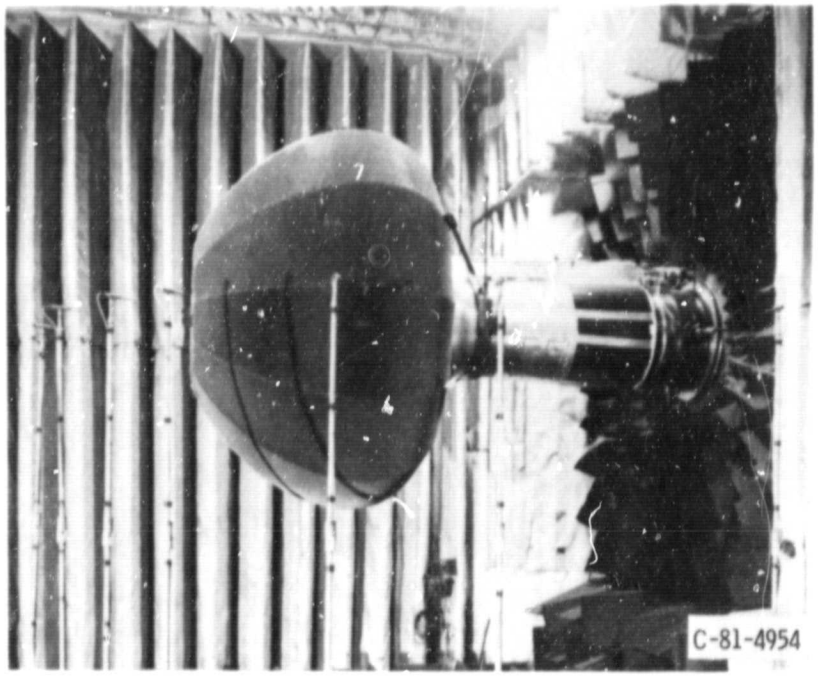

Figure 6. - P-inlet installed in Lewis Anechoic Chamber with ICD inplace.

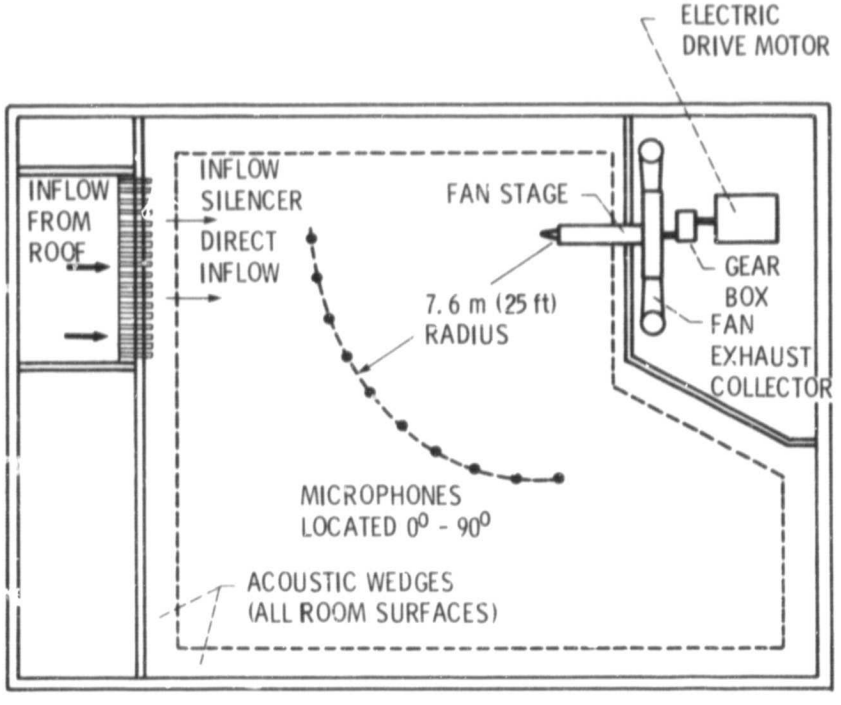

Figure 7. - Plan view of anechoic chamber.

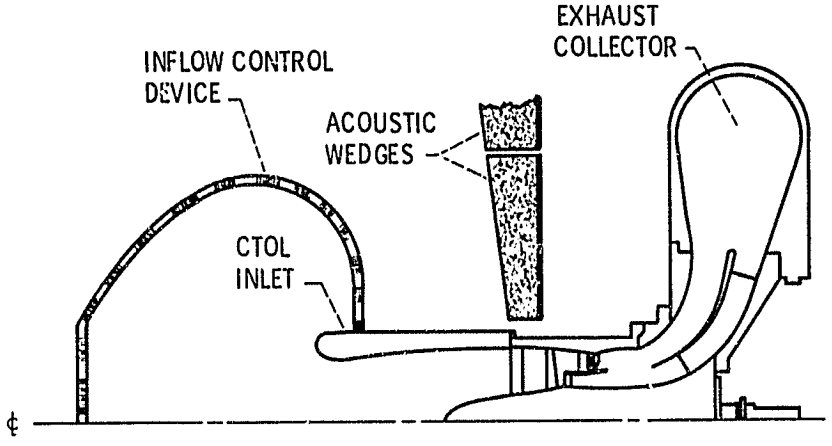

Figure 8. - Cross-sectional view of JT8D refan with CTOL inlet as tested in the anechoic chamber.

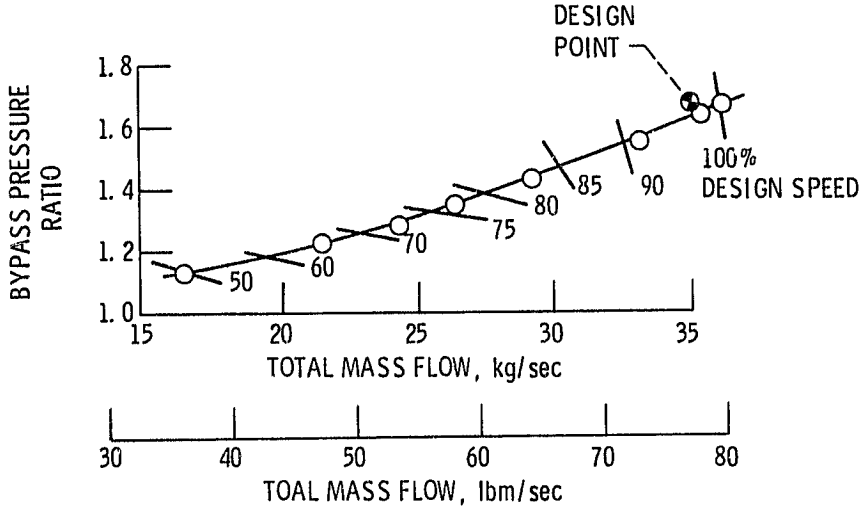

Figure 9. - JT8D refan stage operating map.

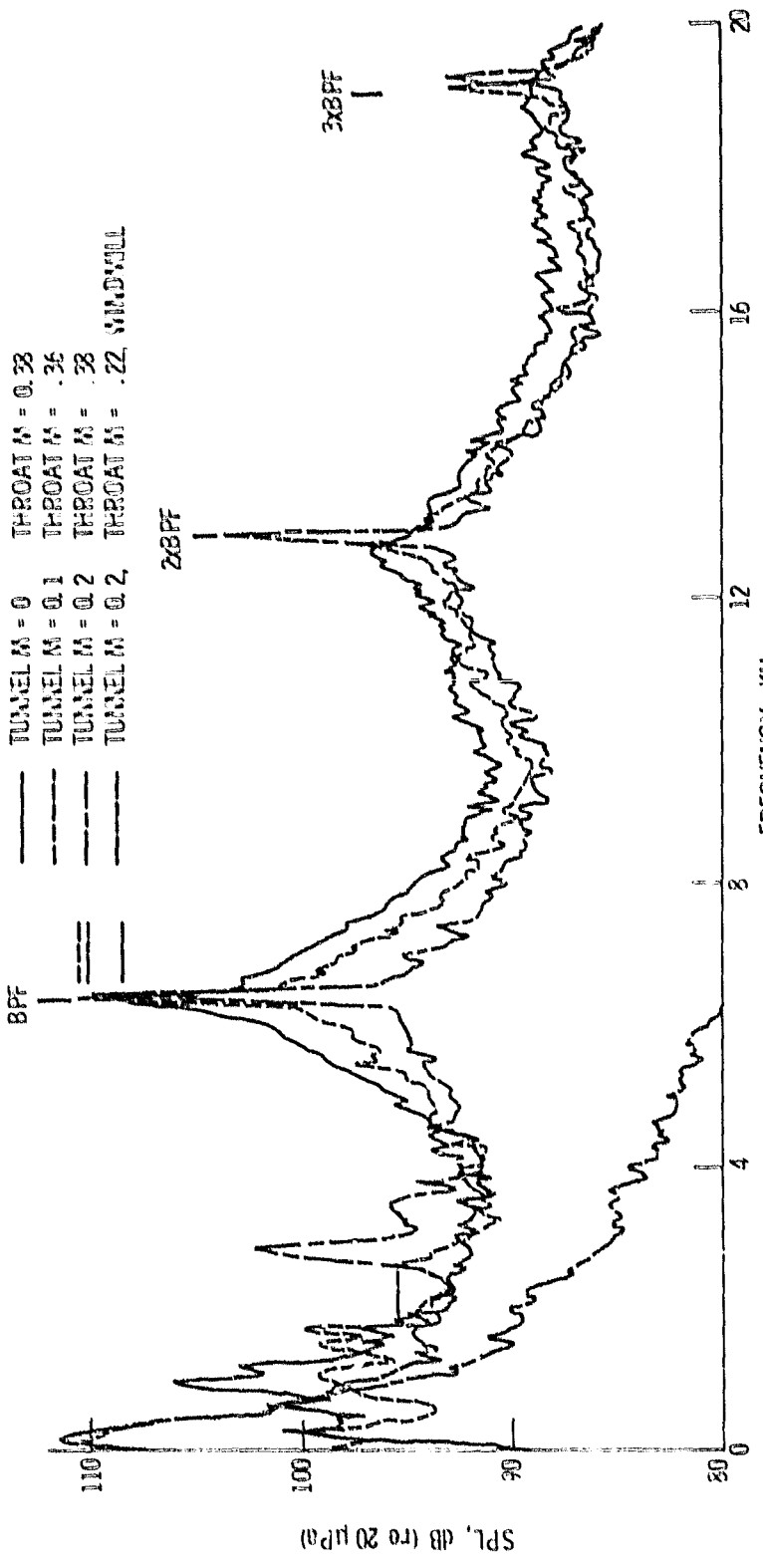

Figure 10 - Effect of tunnel mach number on far field spectra (60% design speed, 70° from inlet axis, centerbody fully extended, 40% open auxiliary doors, both bleeds closed.

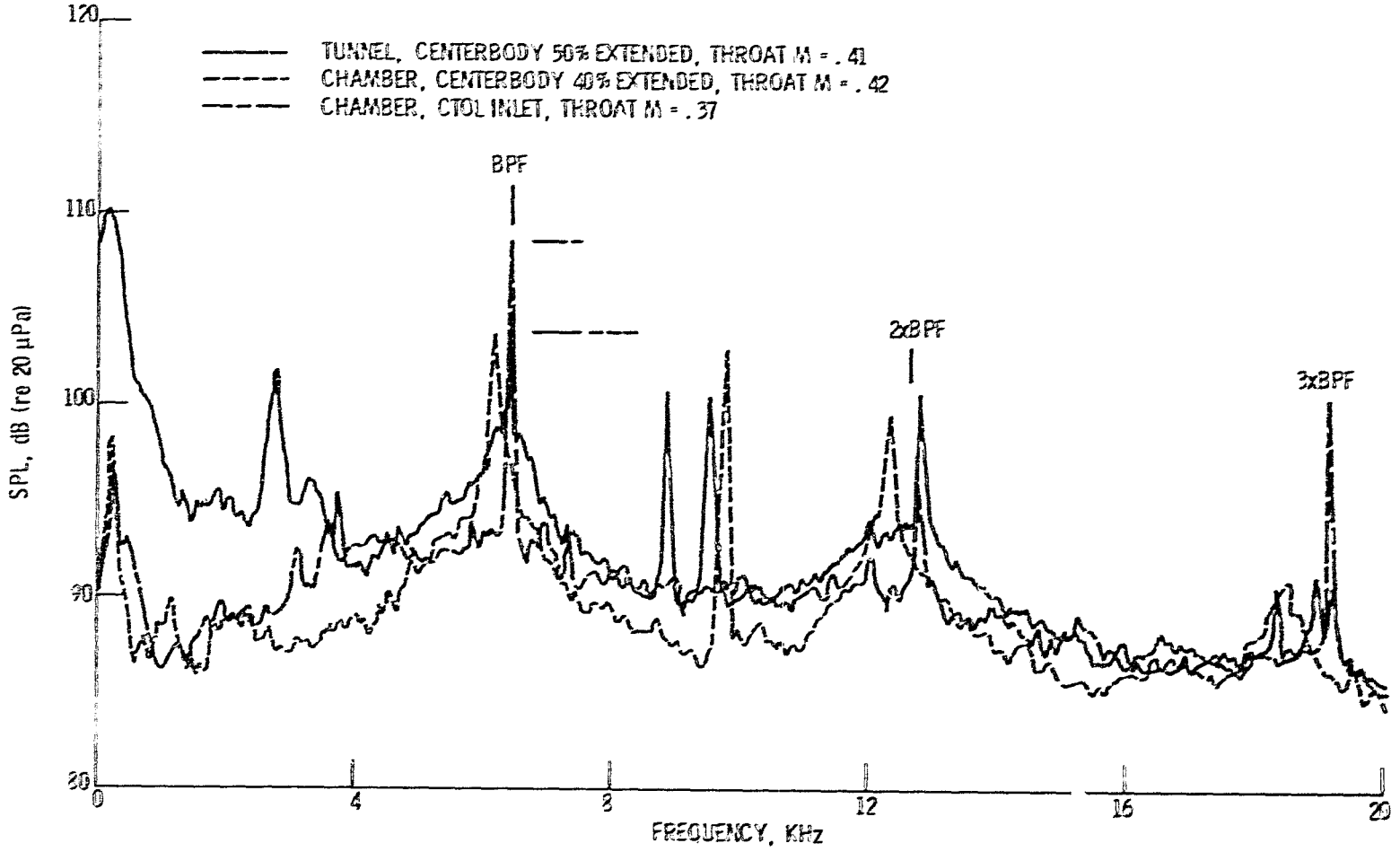

Figure 11 - Comparison of SPL spectra for tunnel and chamber facilities (60% design speed, 70° from inlet axis, 40% open doors, both bleeds closed, data adjusted for 1.83 m radius, tunnel M = .2)

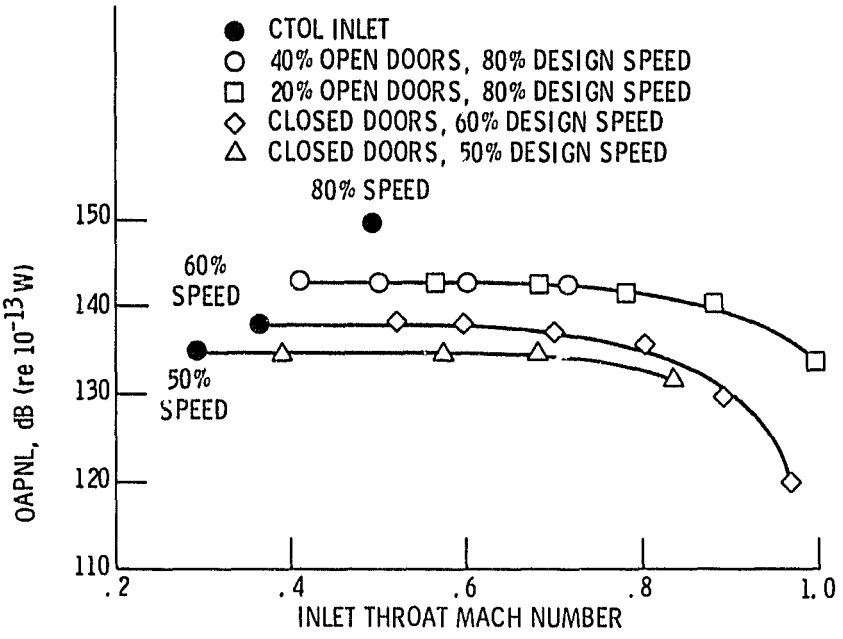

Figure 12. - Overall sound power level (0^0 - 90^0, 1 K - 20 KHz) as a function of throat mach number (anechoic chamber results, P-inlet bleeds closed).

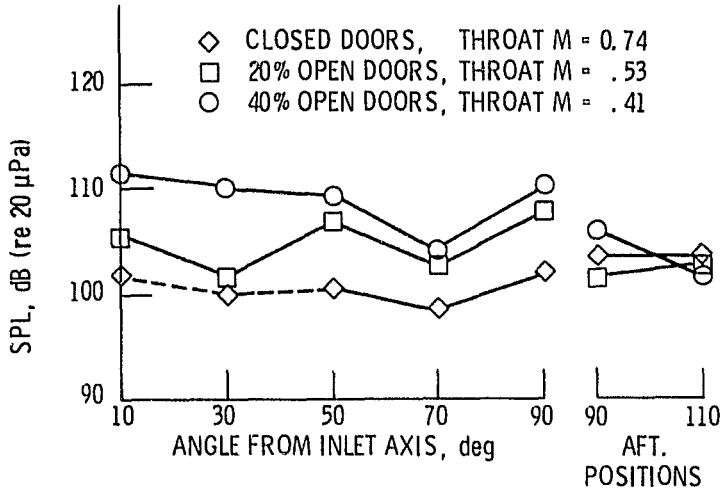

Figure 13. - Blade passage tone directivity for tunnel facility (60% design speed, centerbody 50% extended, bleeds closed, 1.83 m radius).

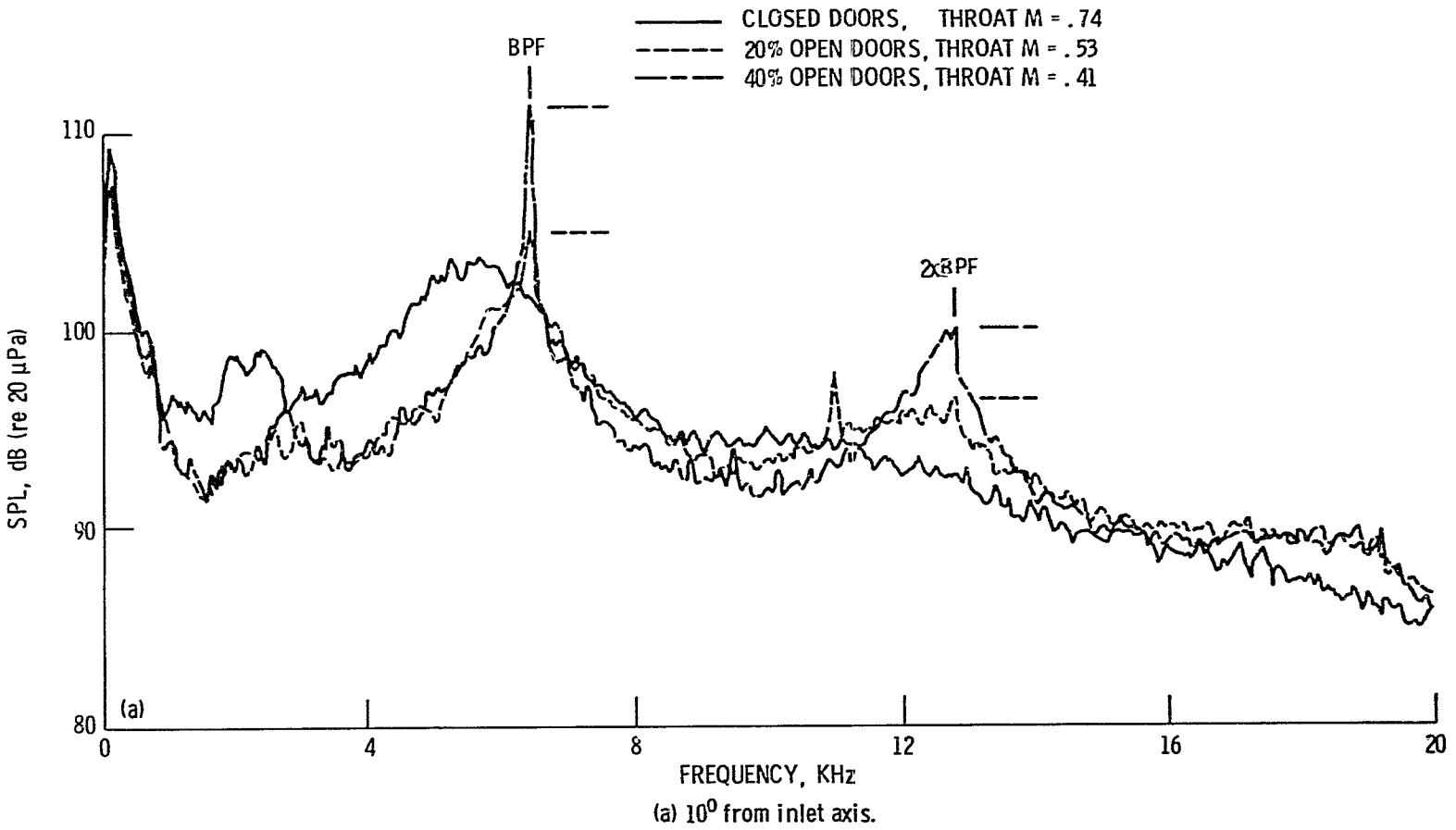

(a) 10^0 from inlet axis.

Figure 14 - Effect of auxiliary door opening on far field spectra with bleeds closed (60% design speed, centerbody 50% extended, tunnel M = .2).

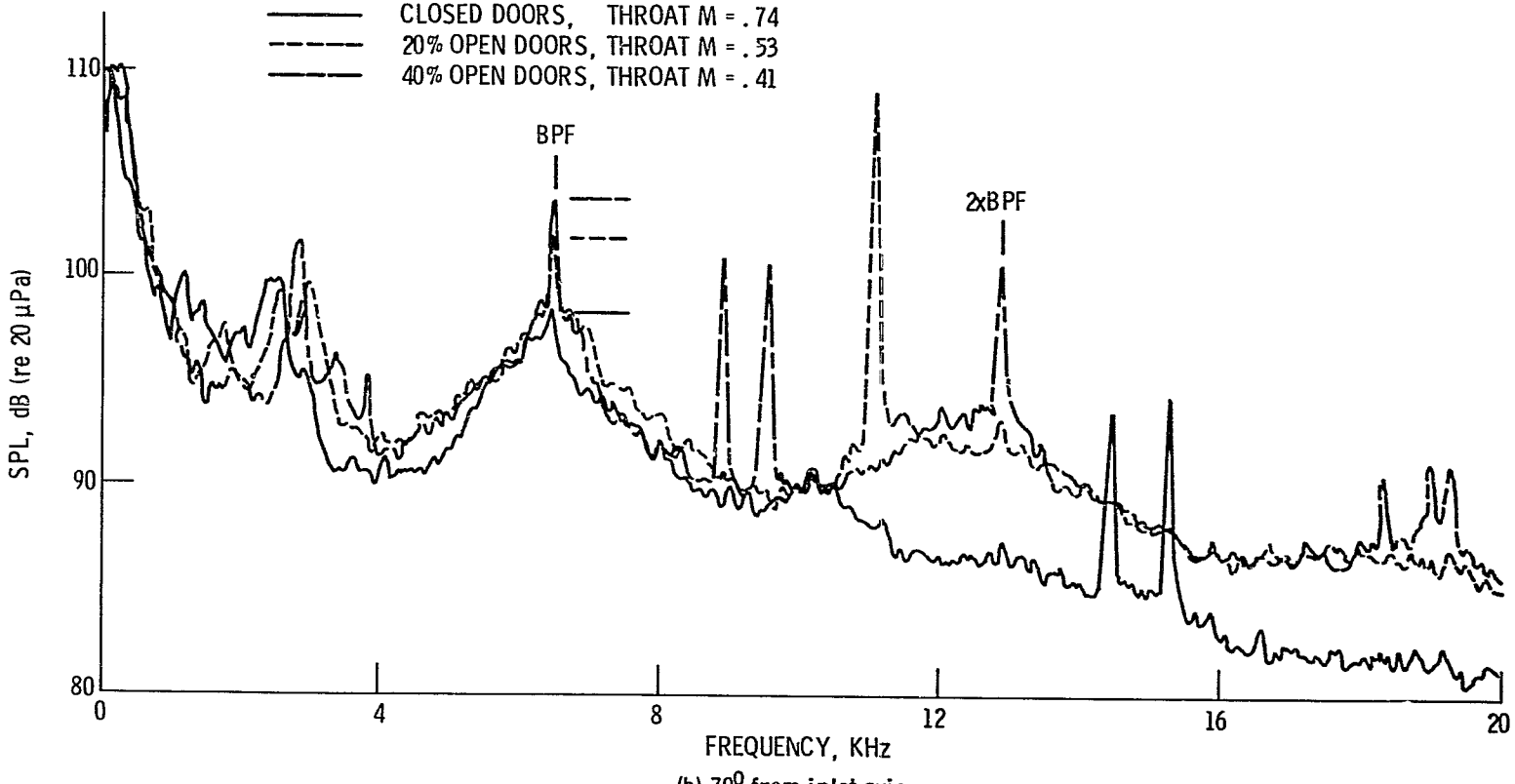

(b) 70^0 from inlet axis.

Figure 14 - Concluded.

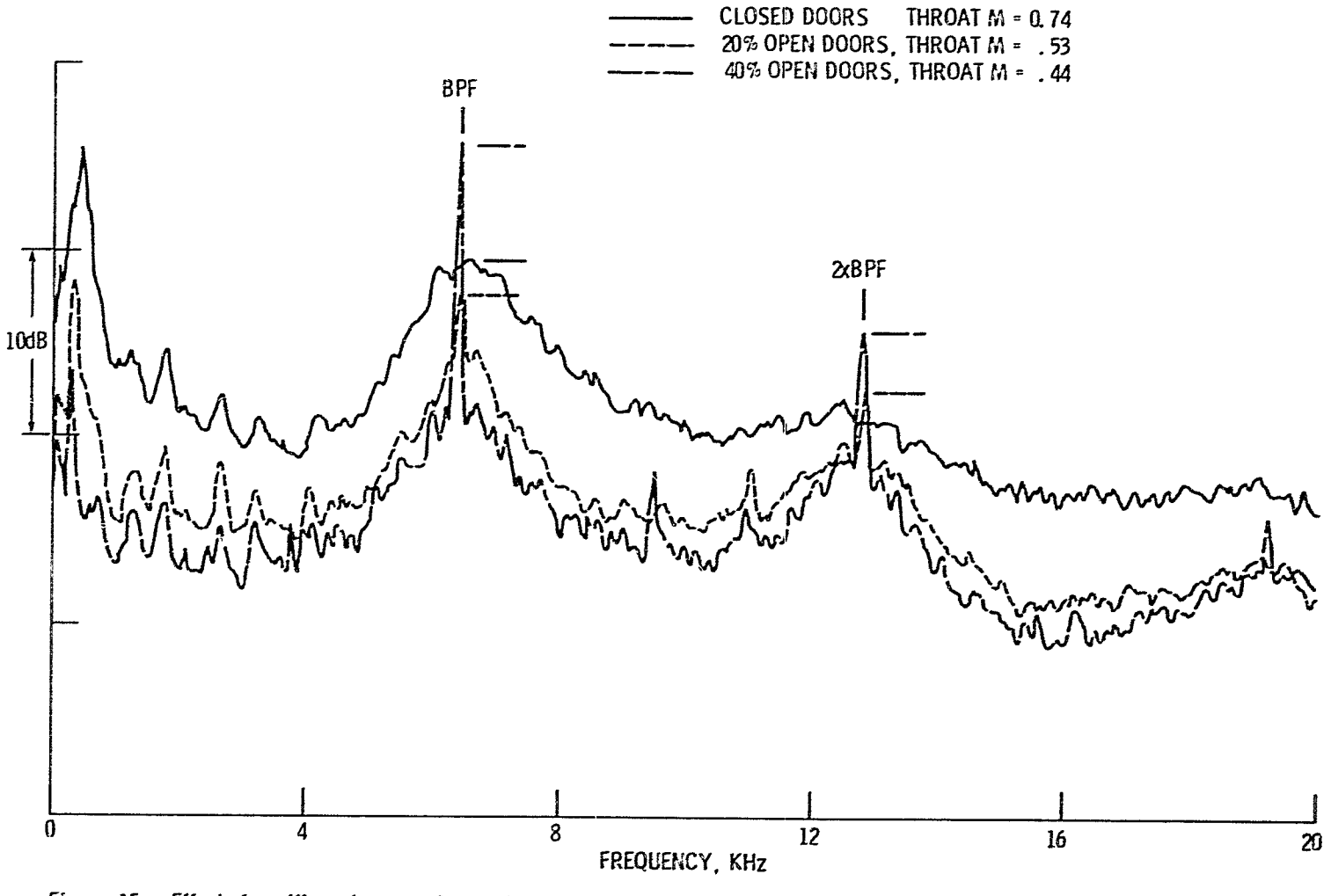

Figure 15. - Effect of auxiliary door opening on internal pressure spectra with bleeds closed (60% design speed, internal duct O.D. just downstream of doors, centerbody 50% extended).

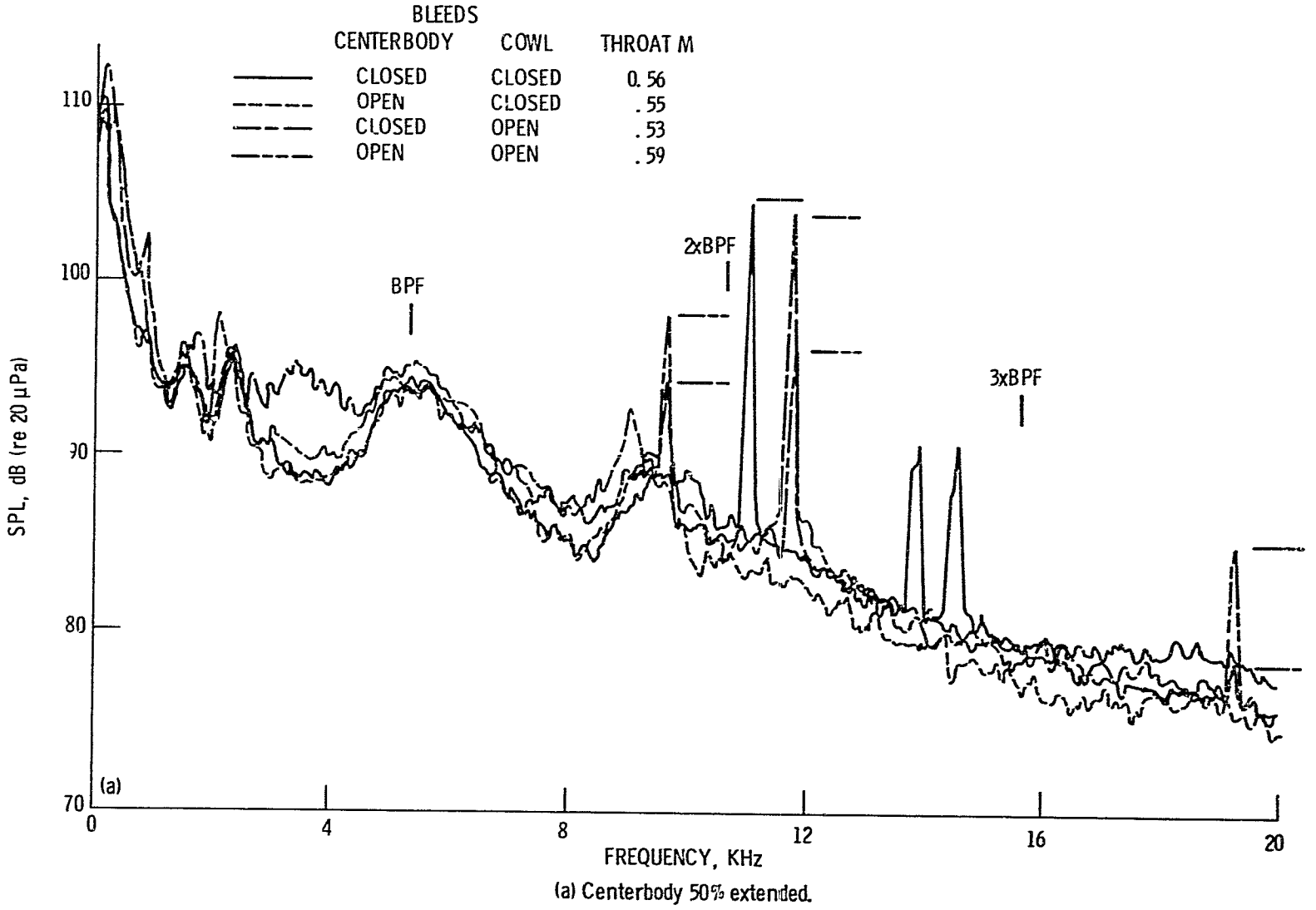

(a) Centerbody 50% extended.

Figure 16. - Effect of inlet bleed configuration on resonance tones in the far field. (Auxiliary doors closed, 50% design speed, 70° from inlet axis).

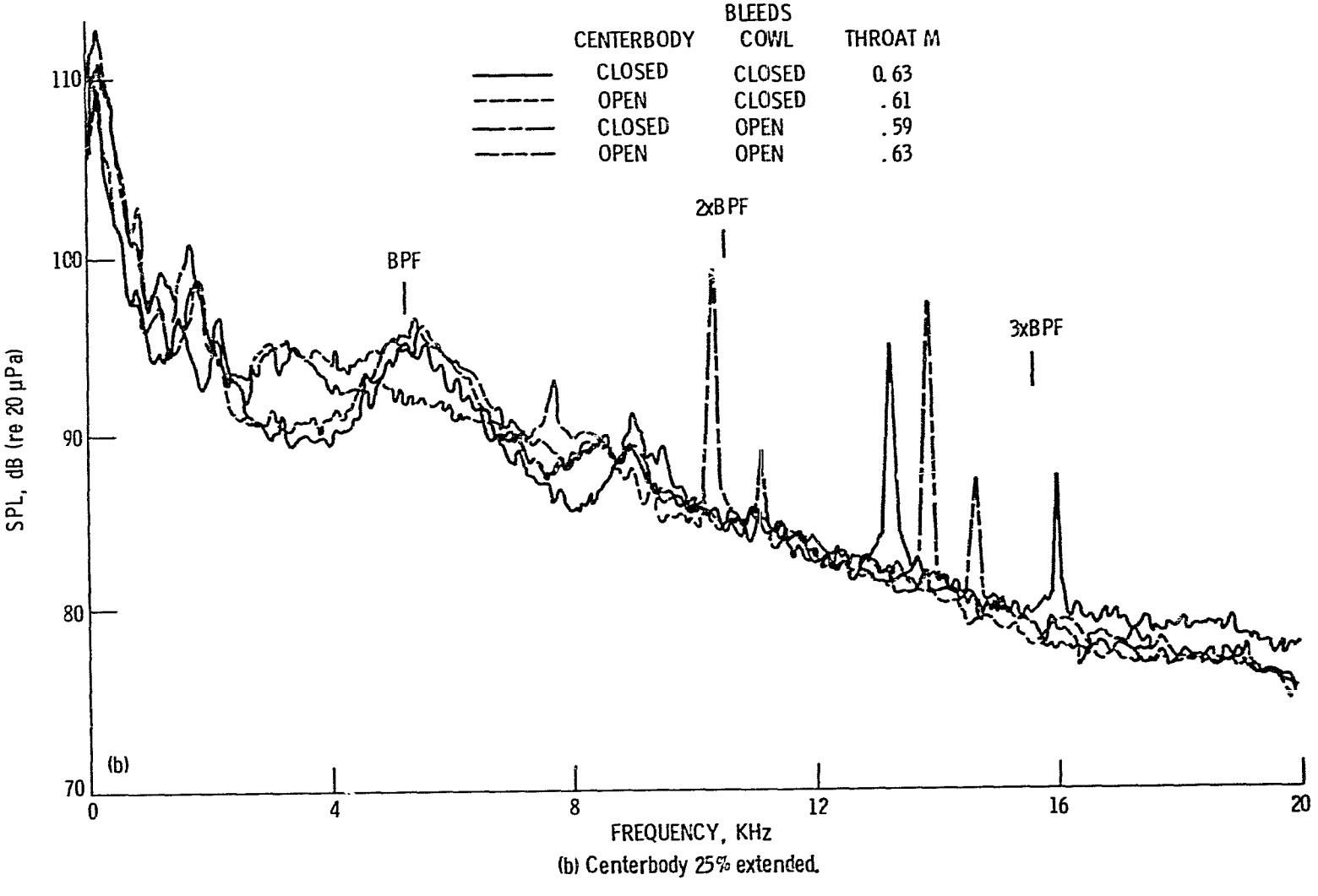

(b) Centerbody 25% extended.

Figure 16. - Concluded.

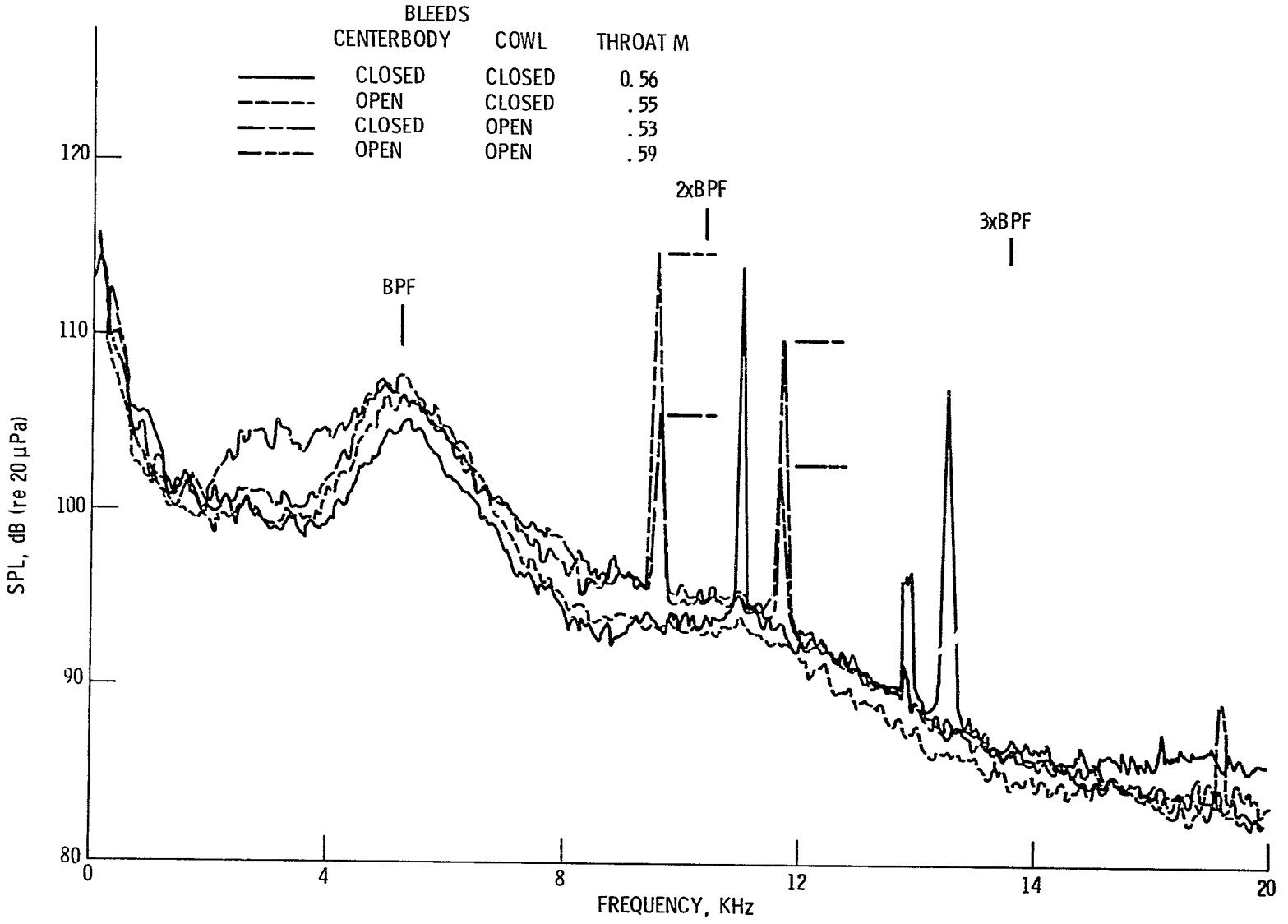

Figure 17. - Effect of bleed configuration on spectra obtained from cowl lip microphone (auxiliary doors closed, 50% design speed, centerbody 50% extended).

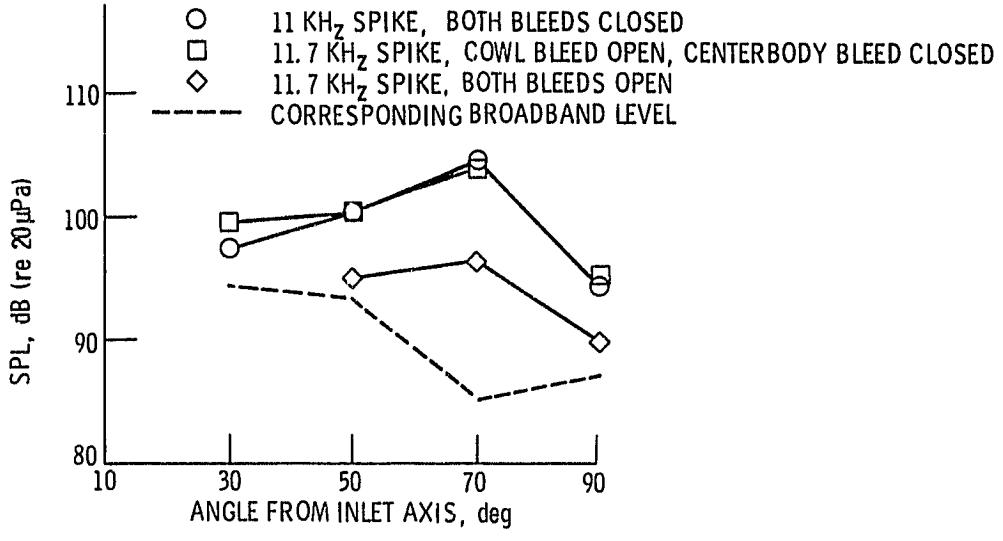

Figure 18. - Resonant tone directivity (50% design speed, closed doors, centerbody 50% extended).

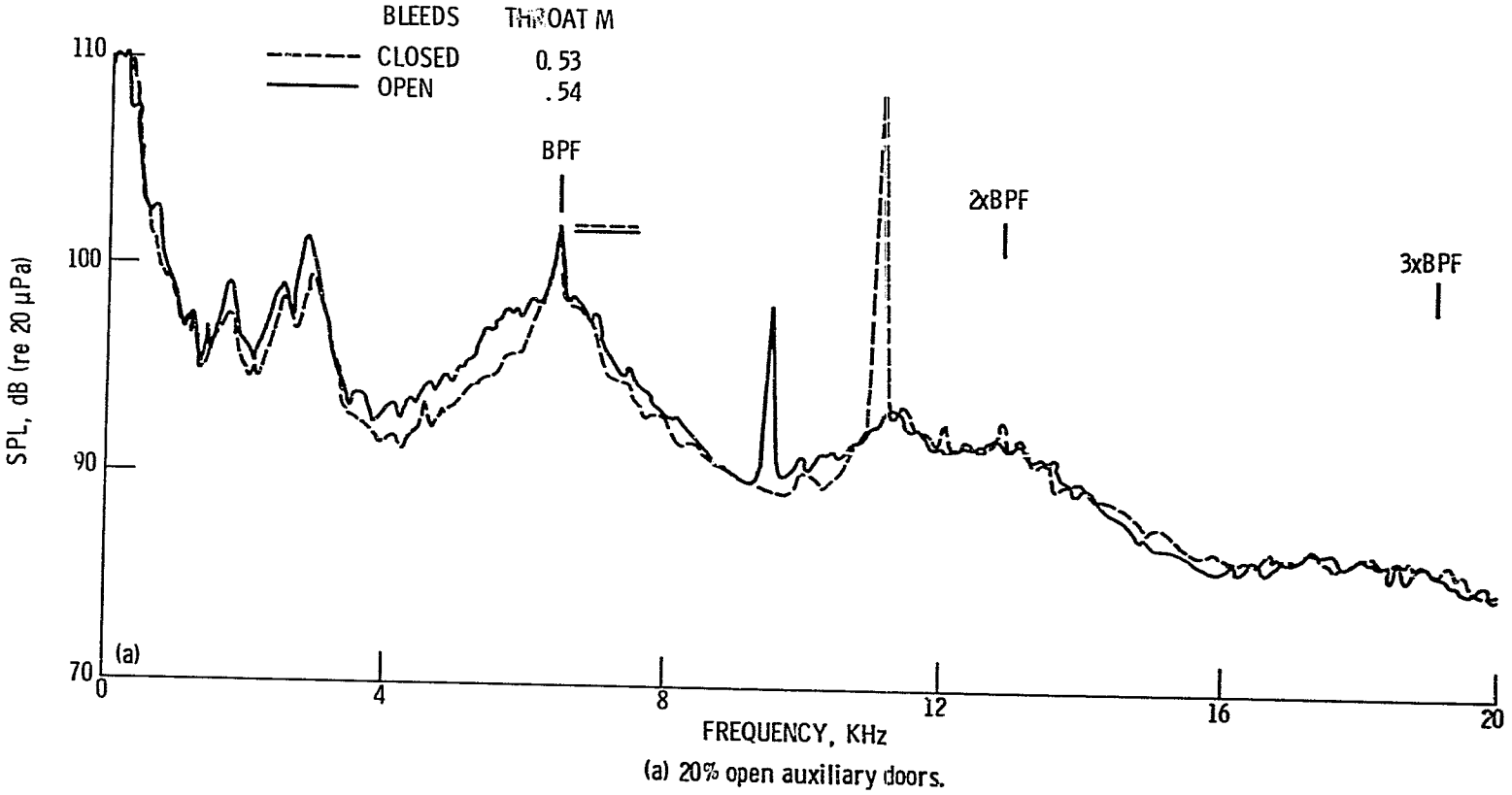

(a) 20% open auxiliary doors.

Figure 19. - Effect of bleed on far field spectra with auxiliary doors open (60% design speed, 70° from inlet axis, centerbody 50% extended).

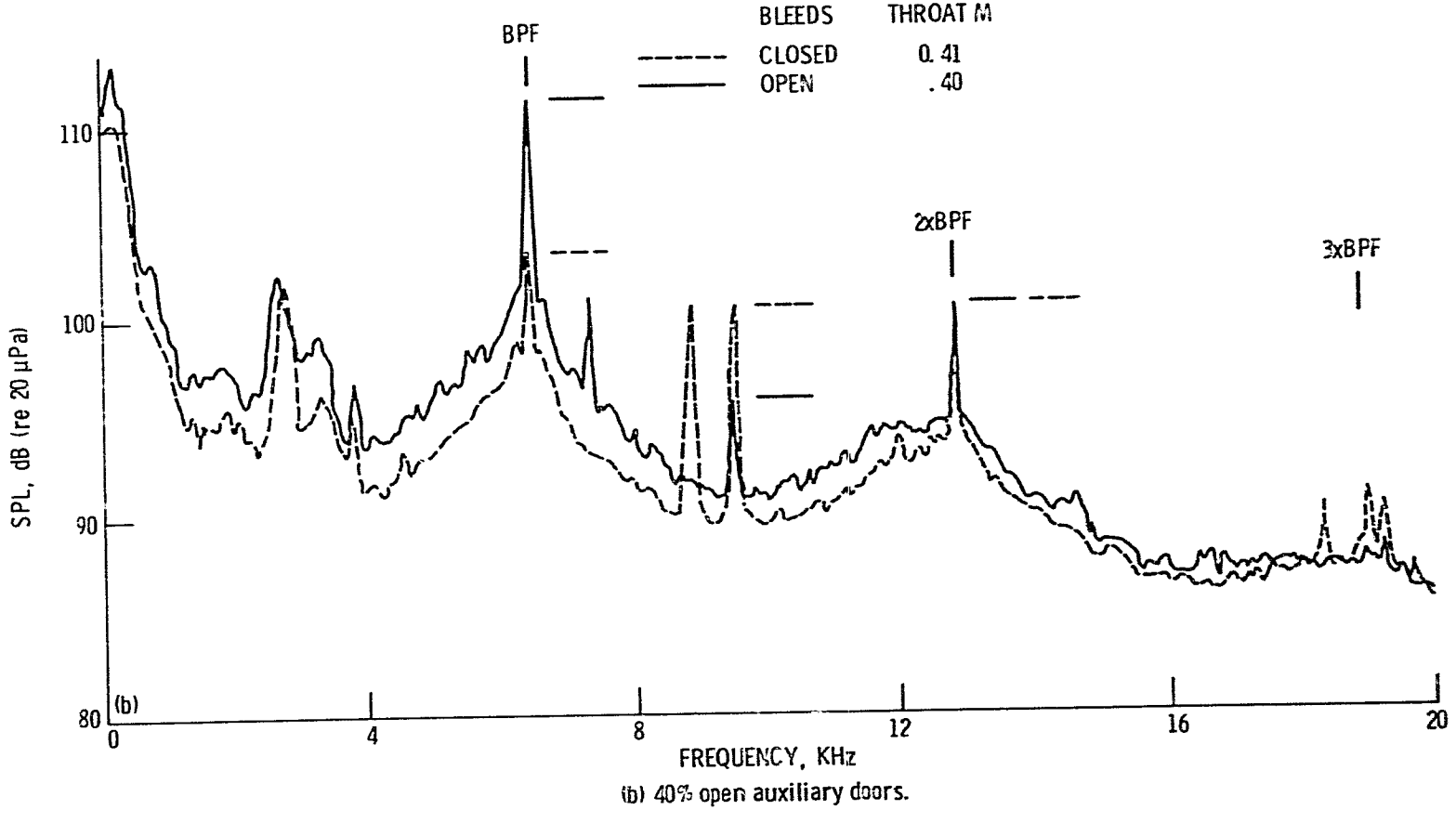

(b) 40% open auxiliary doors.

Figure 19. - Concluded.

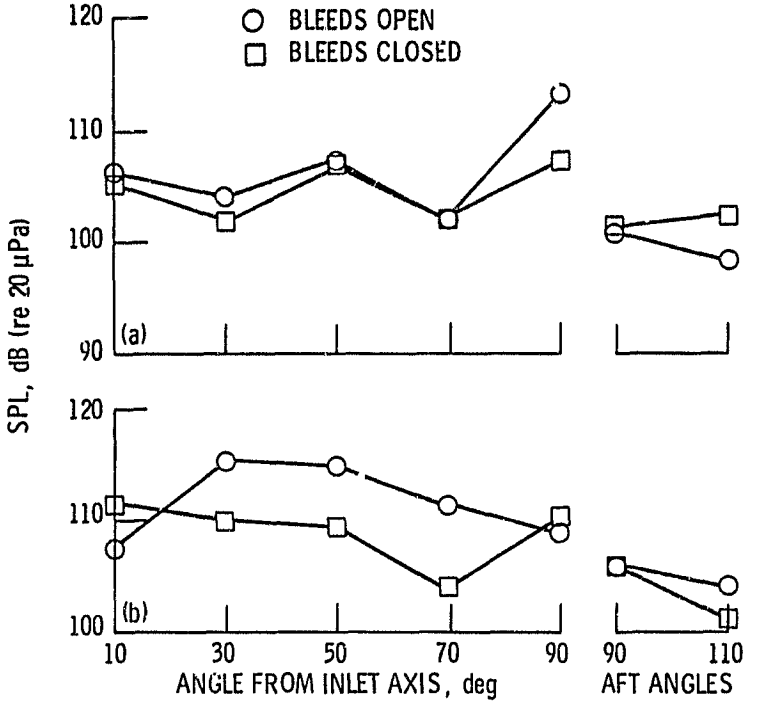

(a) 70% open doors.
(b) 40% open doors.

Figure 20. - Blade passage tone directivity showing effect of bleed and door configurations (60% design speed, centerbody 50% extended).

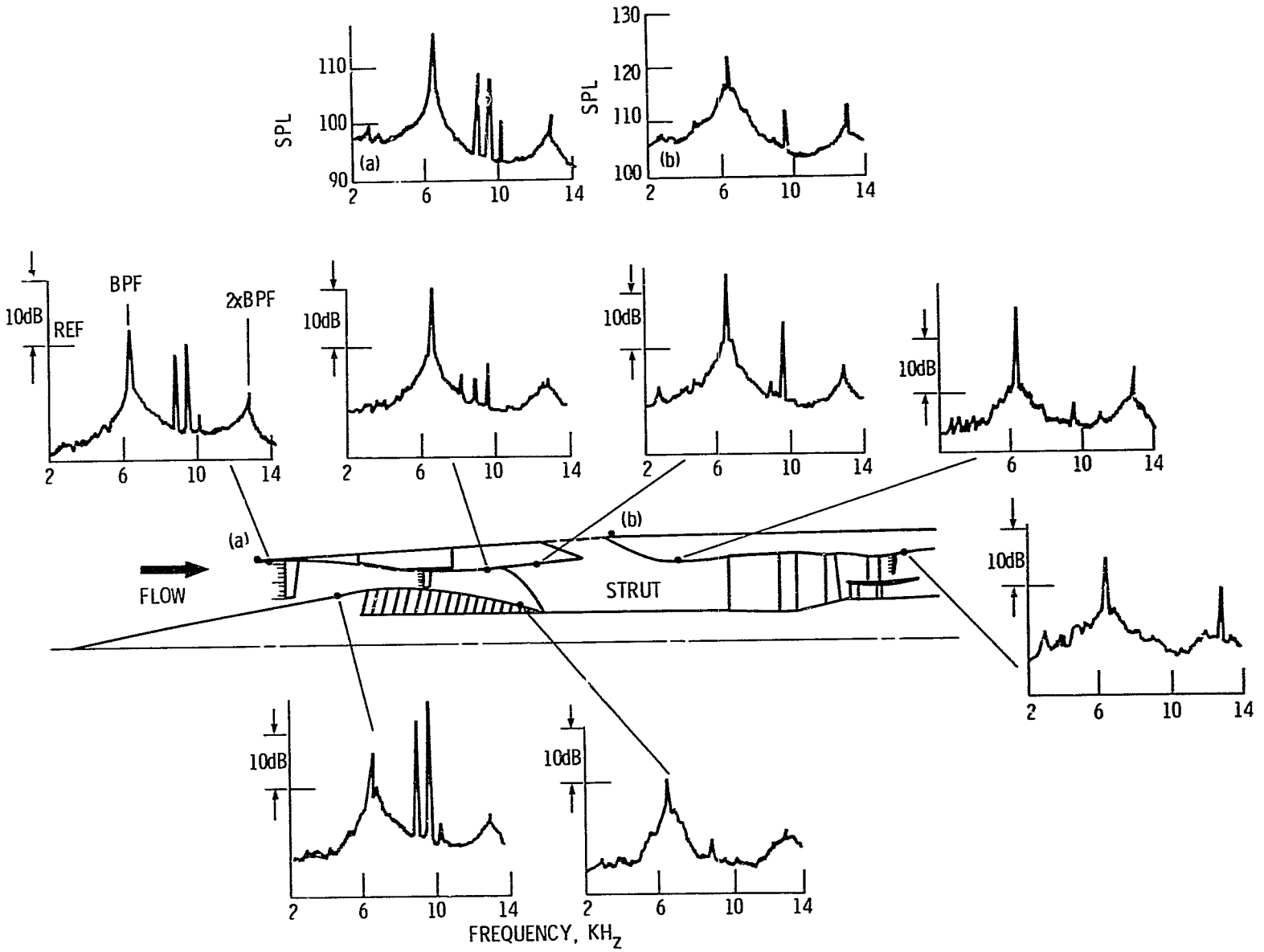

(a) Cowl lip microphone.

(b) Auxiliary door microphone.

Figure 21. - Internal pressure spectra for wind tunnel facility (60% design speed, centerbody 50% extended, 40% open doors, bleeds closed, throat M = .41).

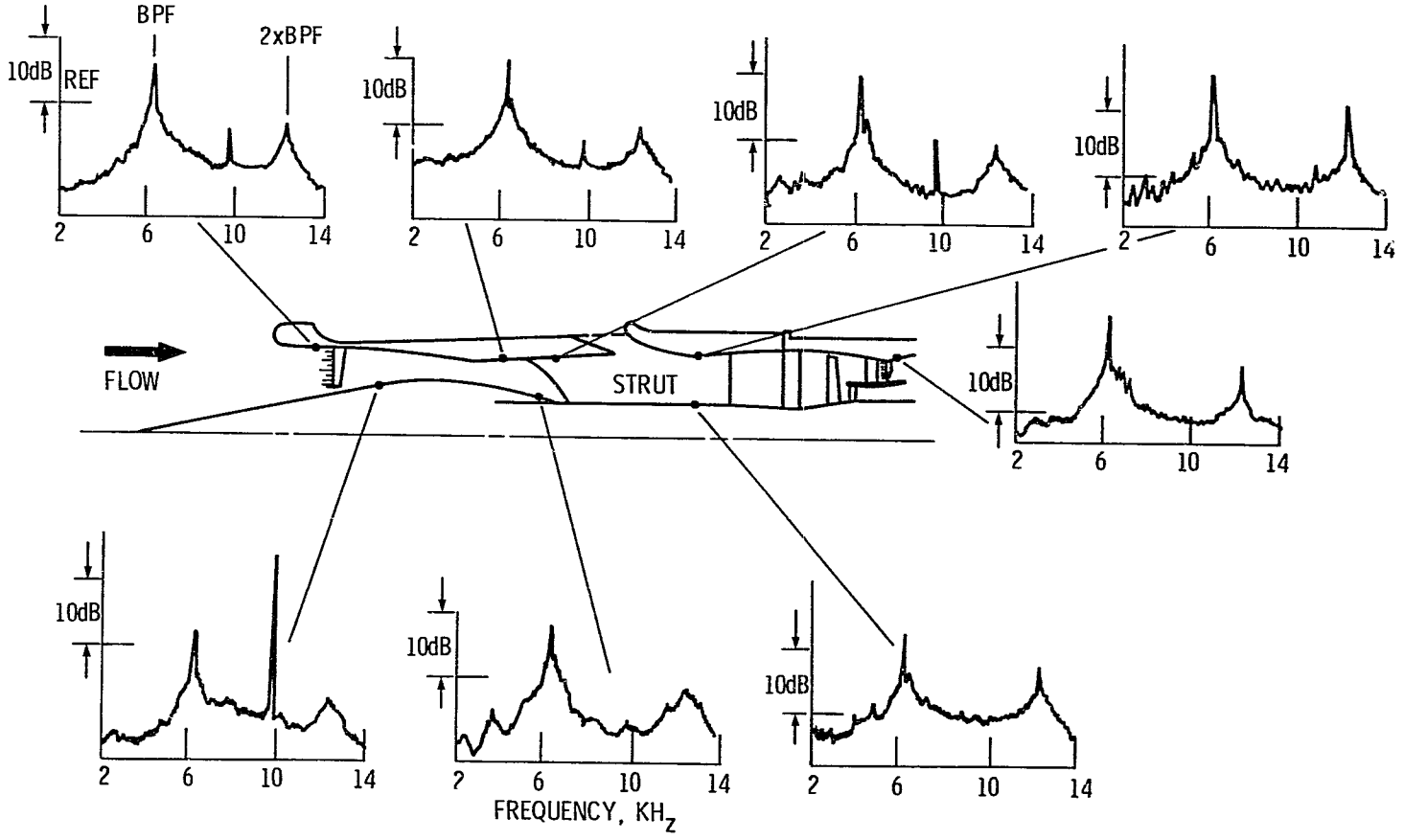

Figure 22. - Internal pressure spectra for chamber facility (60% design speed, centerbody 40% extended, 40% open doors, bleeds closed).

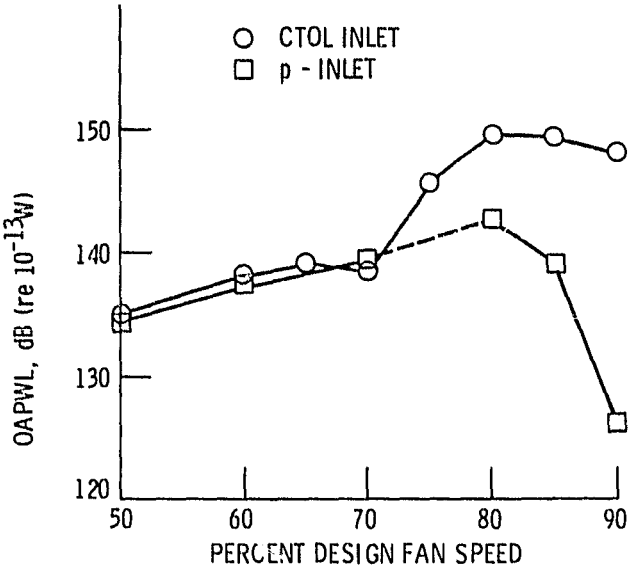

Figure 23. - Overall sound power level (0^0-90^0, 1K - 20KH_z) as a function of fan speed in anechoic chamber (p - inlet: 40% open doors, bleeds closed, centerbody nominal 50% extended).

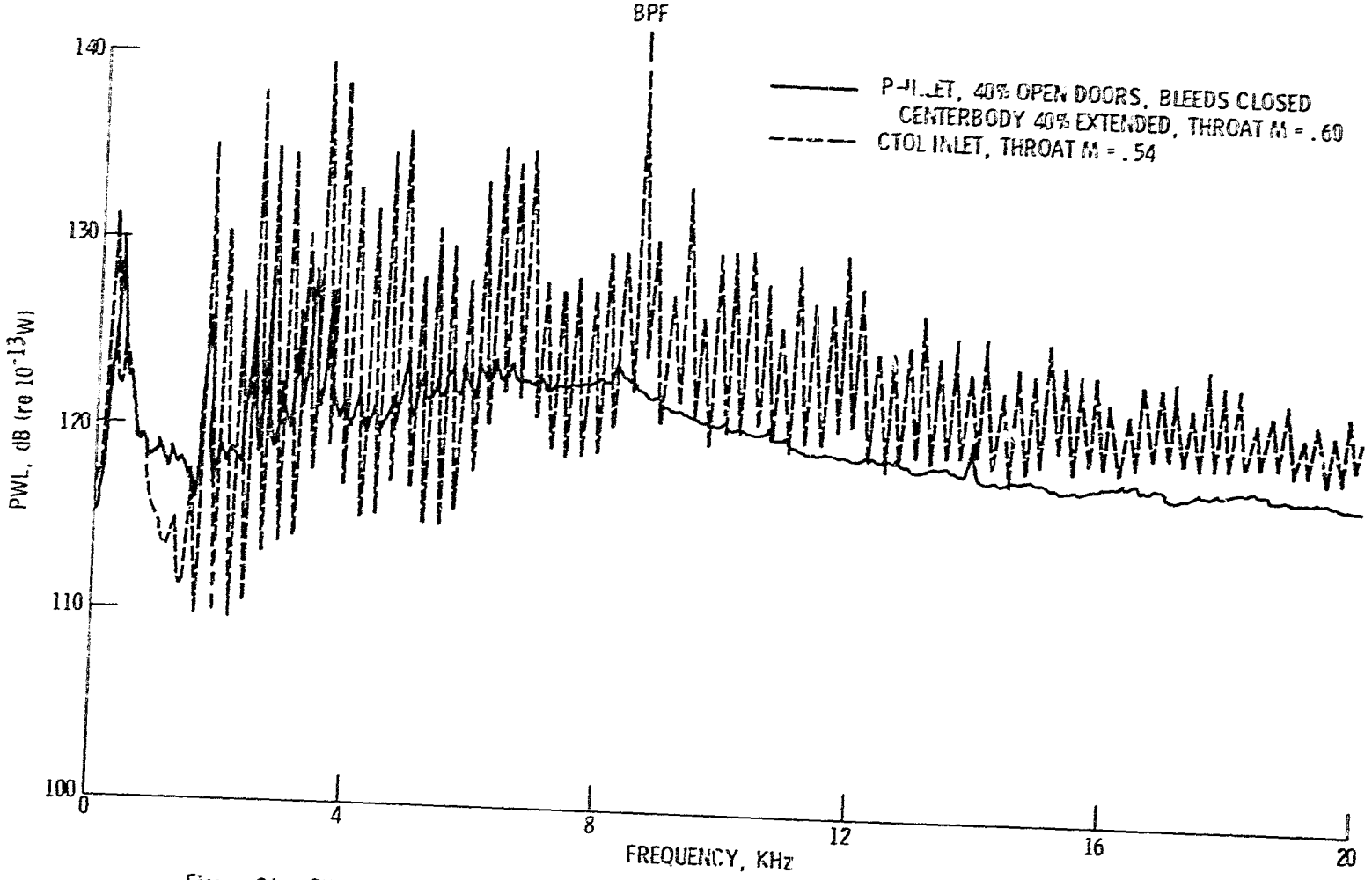

Figure 24 - PWL spectra for P-inlet and CTOL inlet with JT8D refan in anechoic chamber (80% design speed).

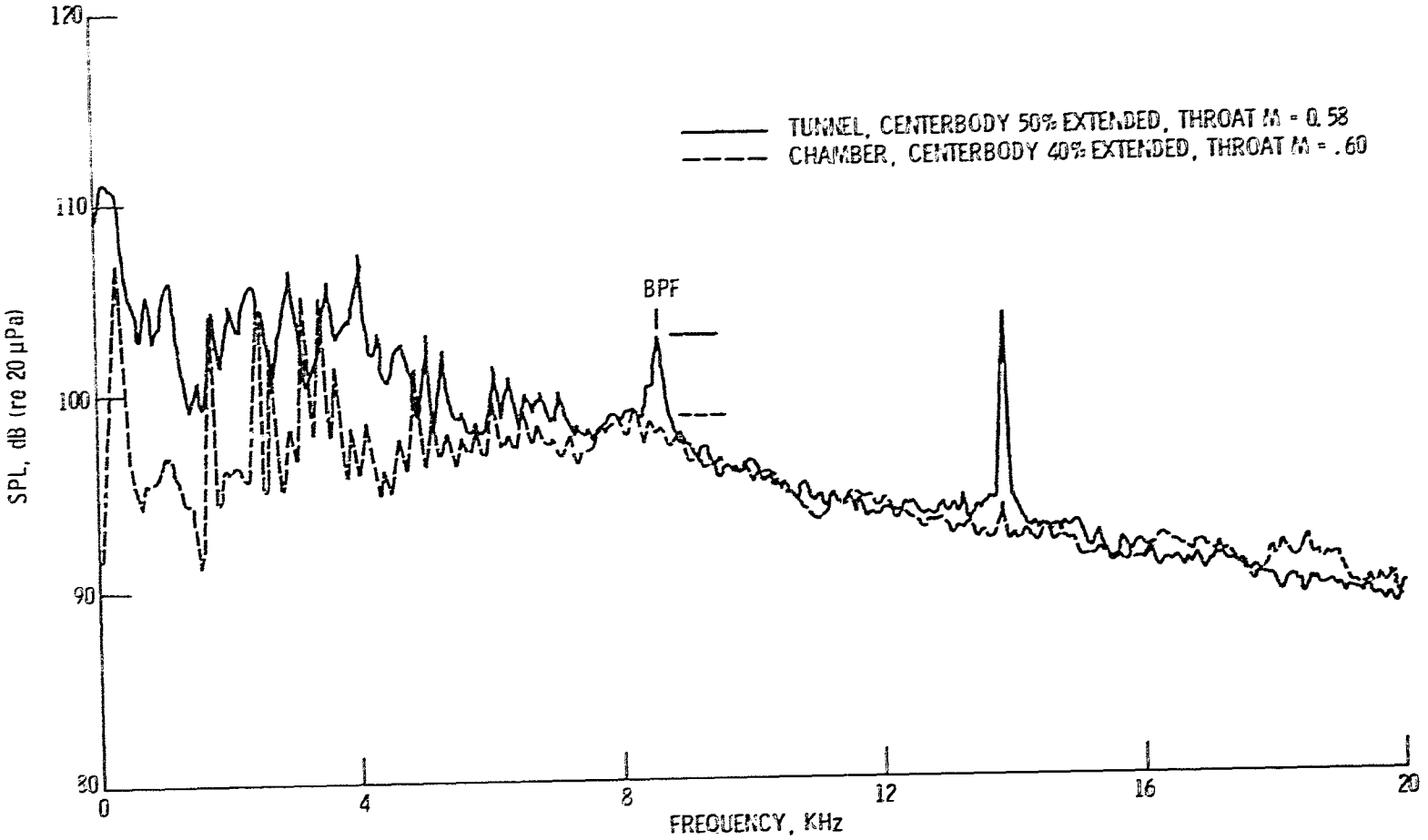

Figure 75. - Comparison of SPL spectra for tunnel and chamber facilities. 80% design speed, 70° from inlet axis, chamber data adjusted for 1.33 M 6 ft radius, 40% open doors, both bleeds closed.

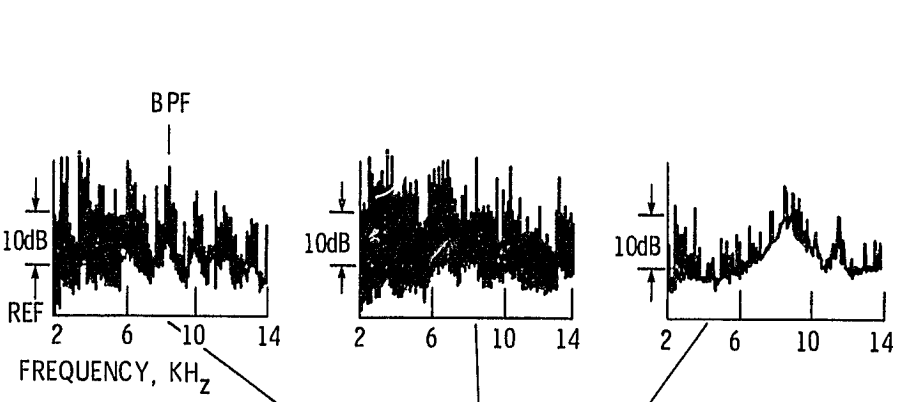

Figure 26. - Internal pressure spectra for JT8D refan in anechoic chamber (80% design fan speed, throat M = .54).

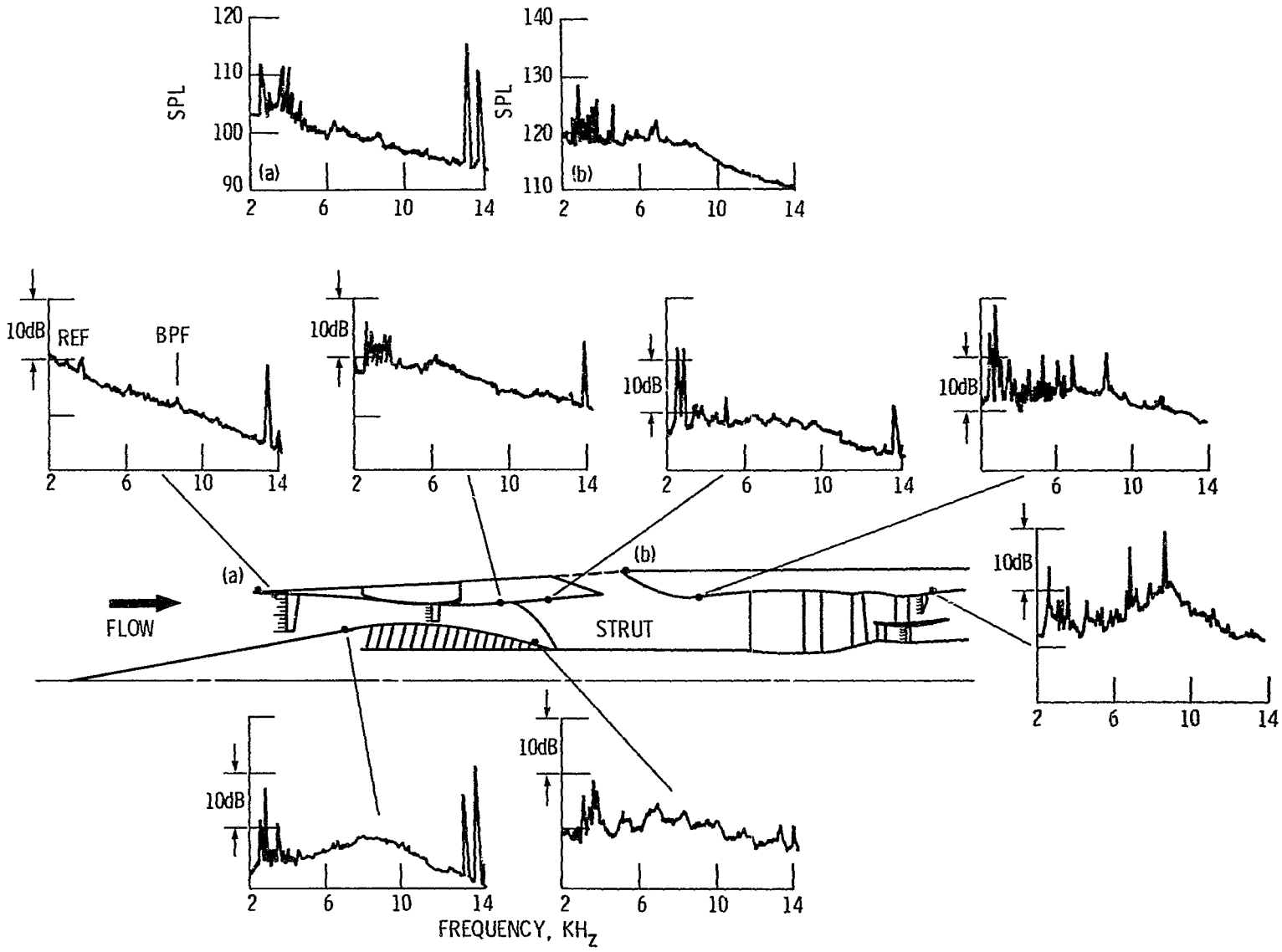

(a) Cowl lip microphone.

(b) Auxiliary door microphone.

Figure 27. - Internal pressure spectra for wind tunnel facility (80% design speed, centerbody 50% extended, 40% open doors, bleeds closed, throat M = .58)

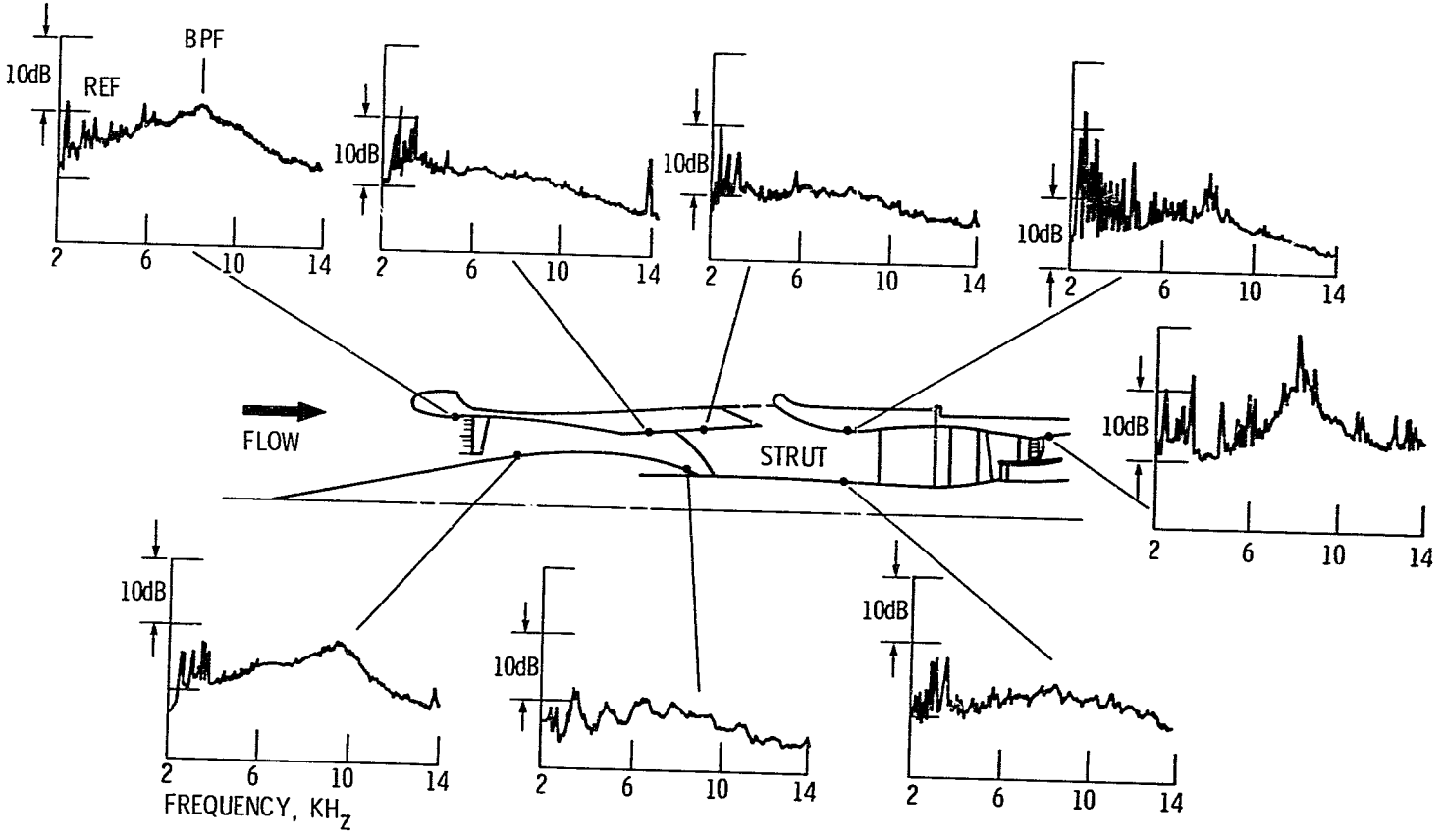

Figure 28. - Internal pressure spectra for chamber facility (80% design speed, centerbody 40% extended, 40% open doors, bleeds closed throat M = .60).

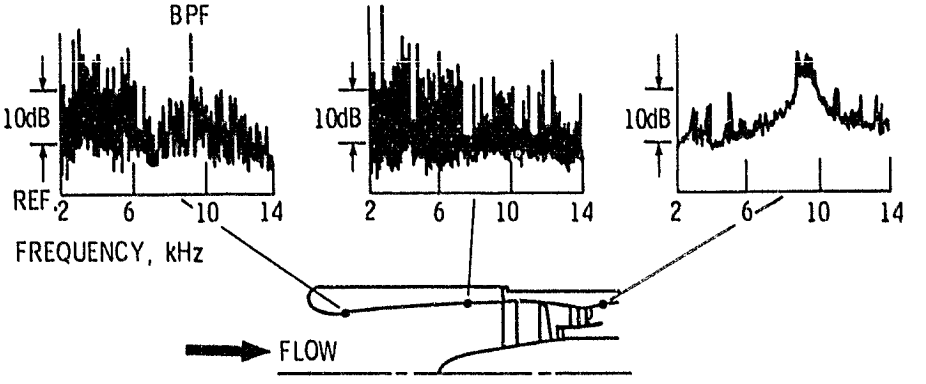

Figure 29. - Internal pressure spectra for JT8D refan in anechoic chamber (90% design speed, throat M ≈ .65).

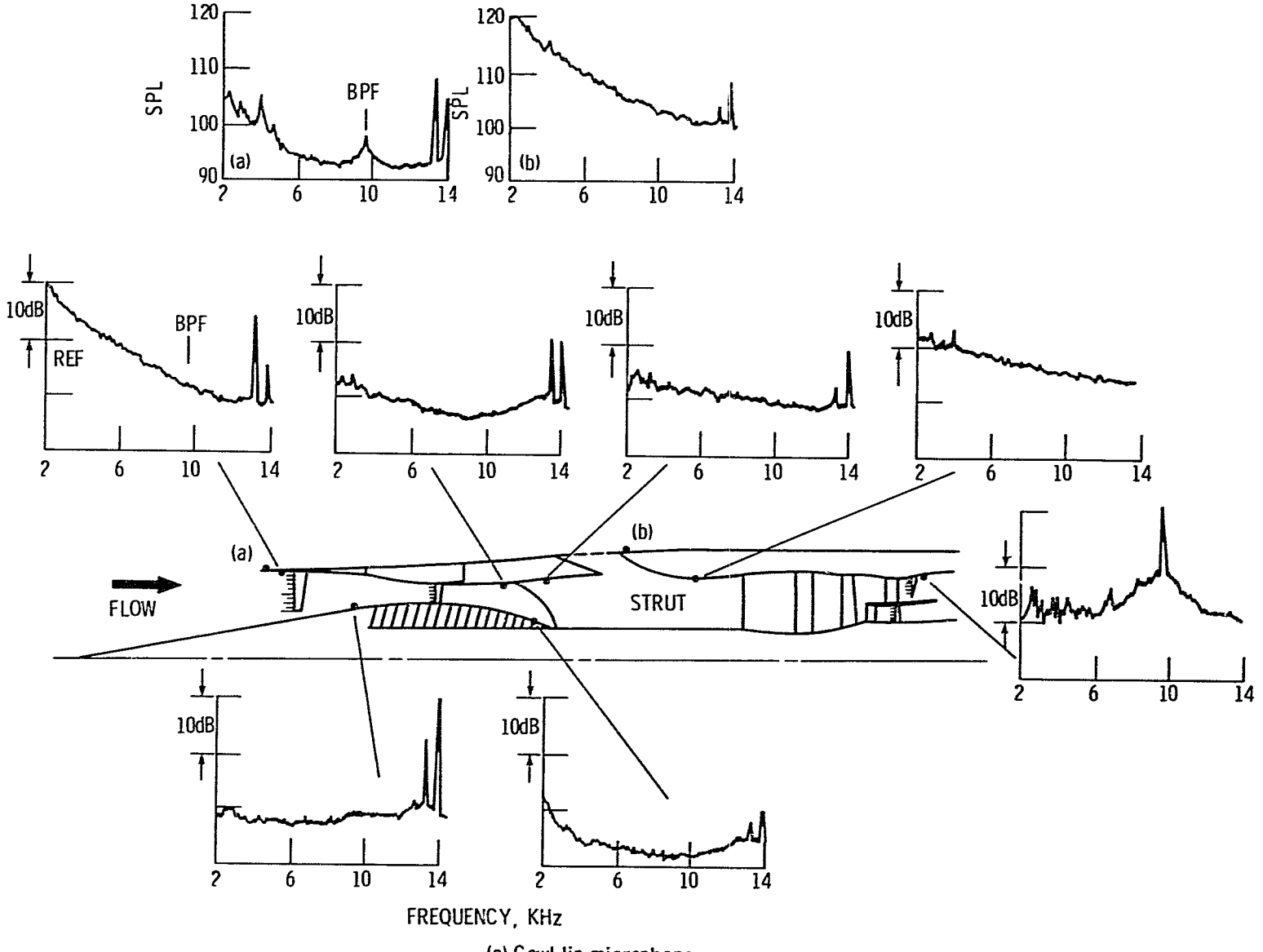

(a) Cowl lip microphone.

(b) Auxiliary door microphone.

Figure 30. - Internal pressure spectra for wind tunnel facility (90% design speed, centerbody 50% extended, 40% open doors, bleeds closed, throat M = .68).

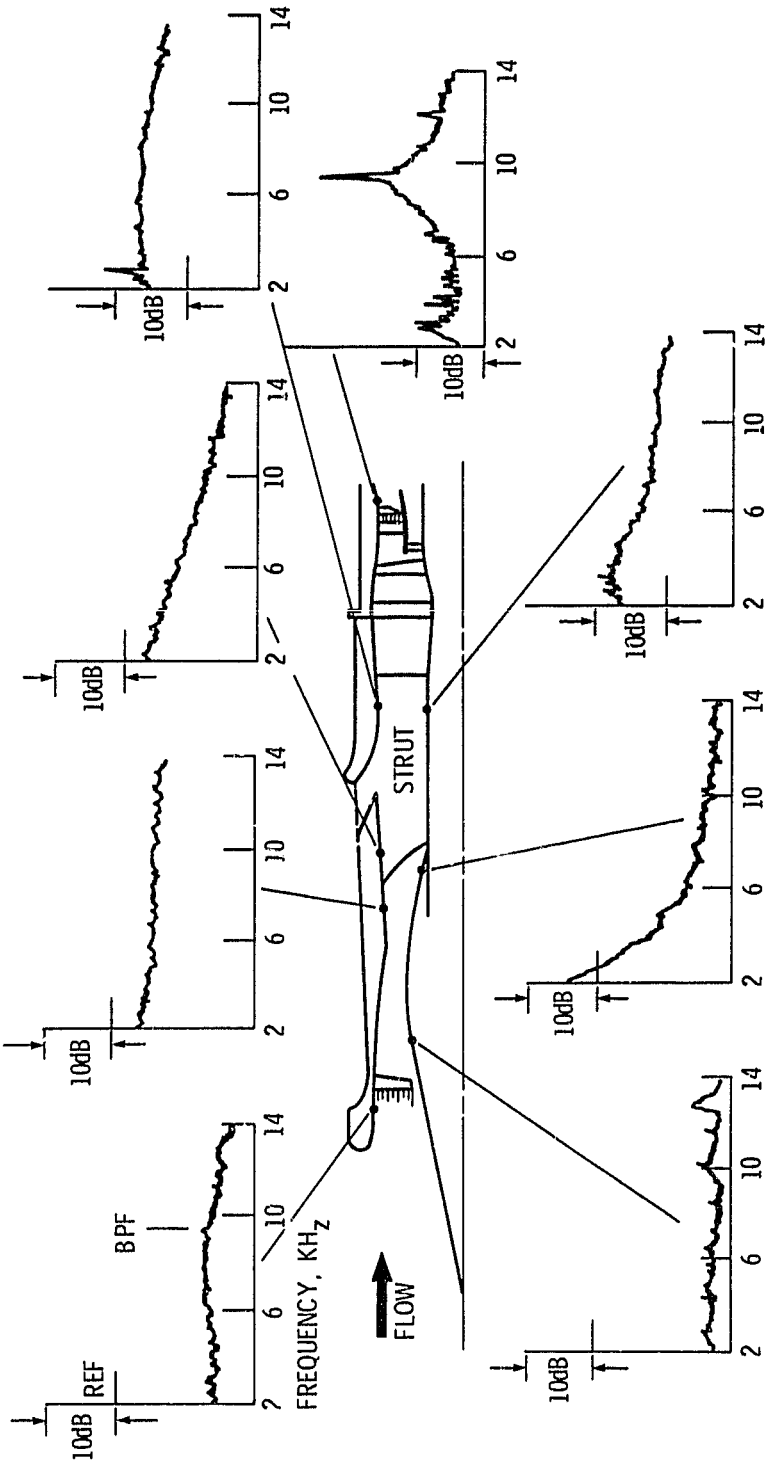

Figure 31. - Internal pressure spectra for chamber facility (90% design speed, centerbody 50% extended, 40% open doors, bleeds closed).

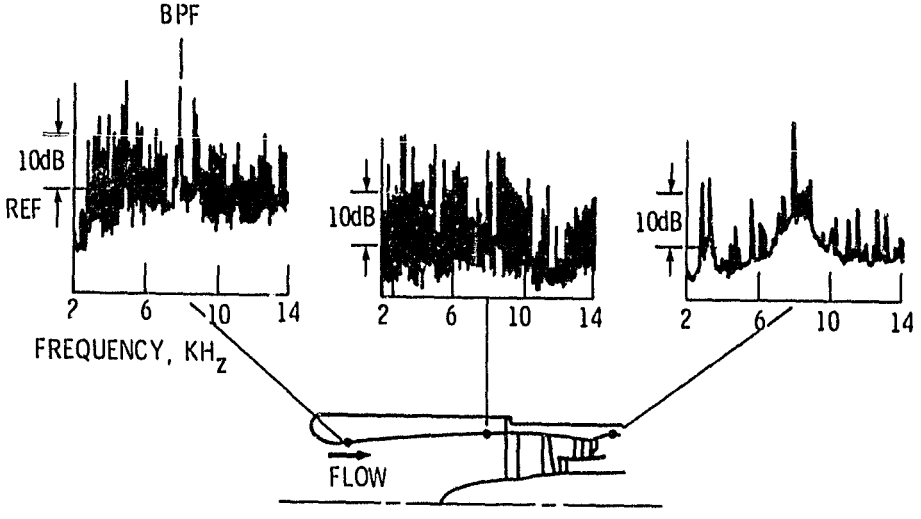

Figure 32. - Internal pressure spectra for JT8D refan in anechoic chamber (75% design fan speed, throat M = .49)

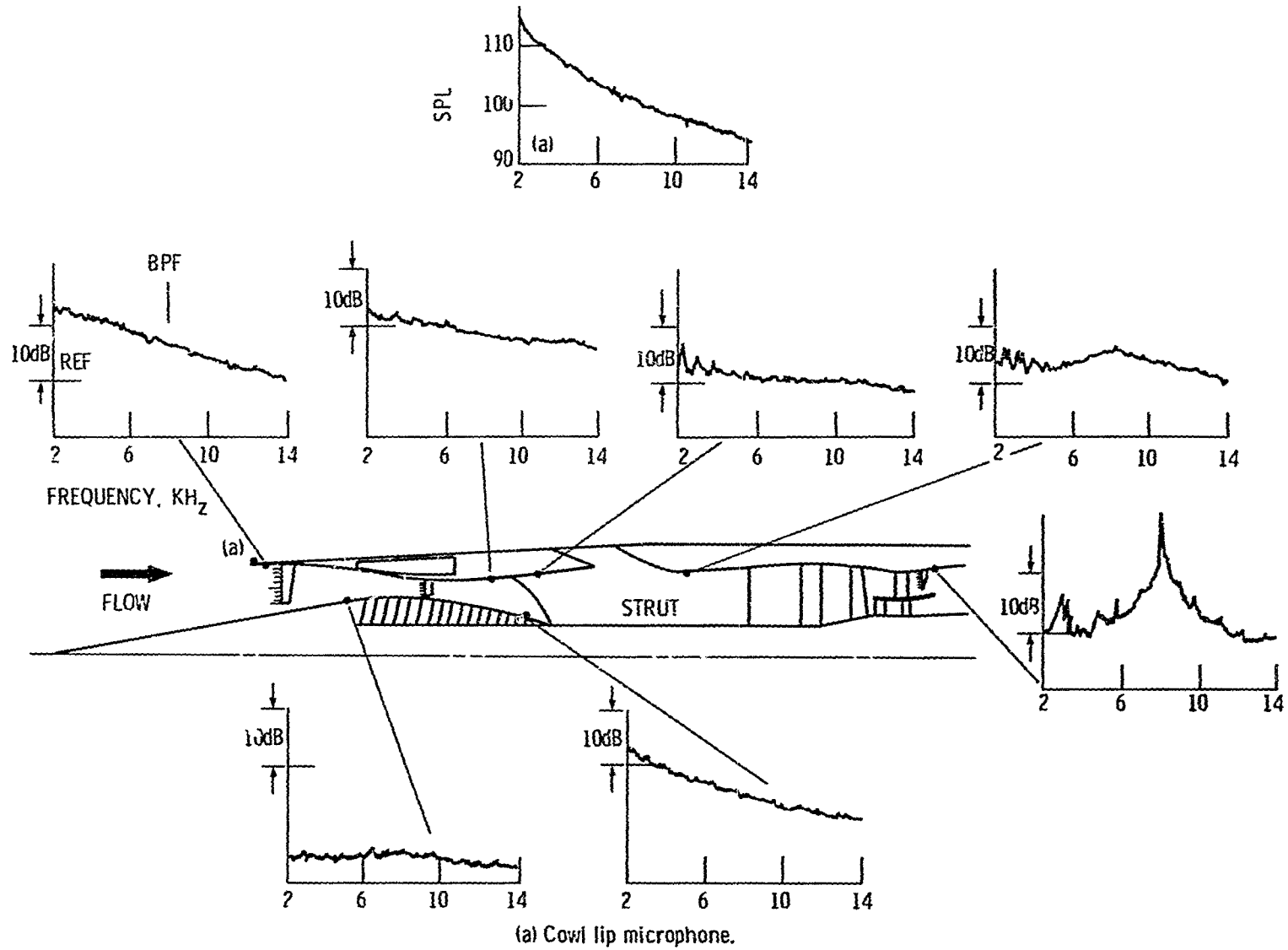

(a) Cowl lip microphone.

Figure 33. - Internal pressure spectra for wind tunnel facility (75% design speed, centerbody 100% extended, doors and bleeds closed, throat M = 1.0).

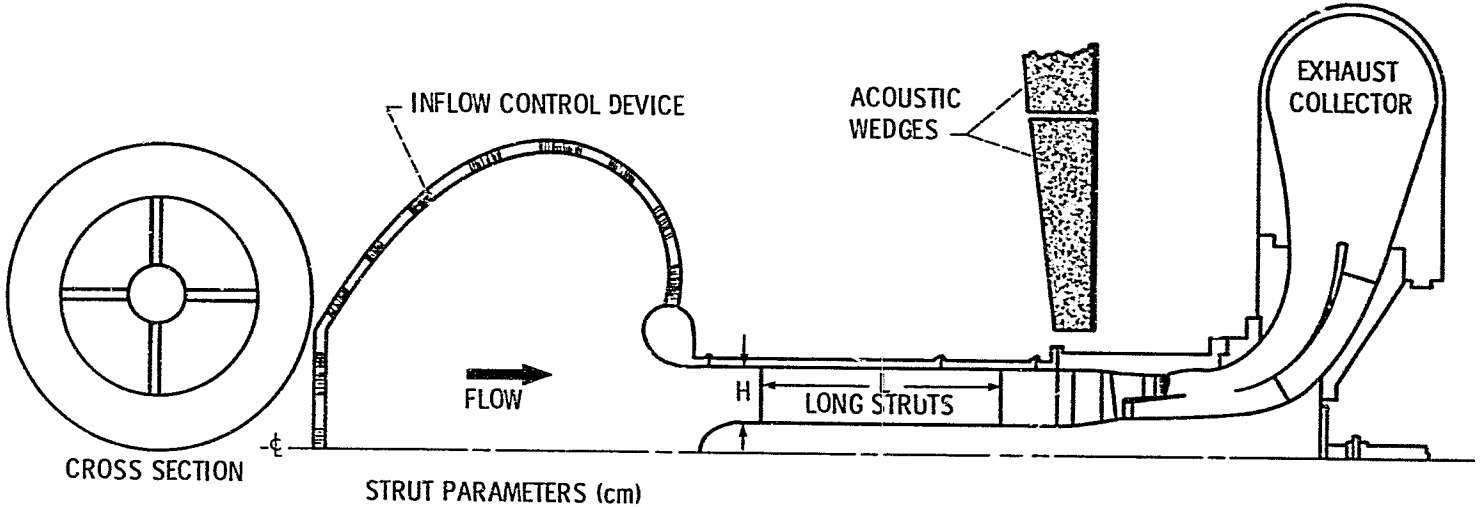

STRUT PARAMETERS (cm)

L/M	M	L	THICKNESS
1.0	17.2	17.2	0.32
2.0		34.3	
4.0		68.6	
8.0		137.2	

Figure 34 - Long inlet strut configuration tested in the anechoic chamber (4 struts at 90° circumferential spacing).

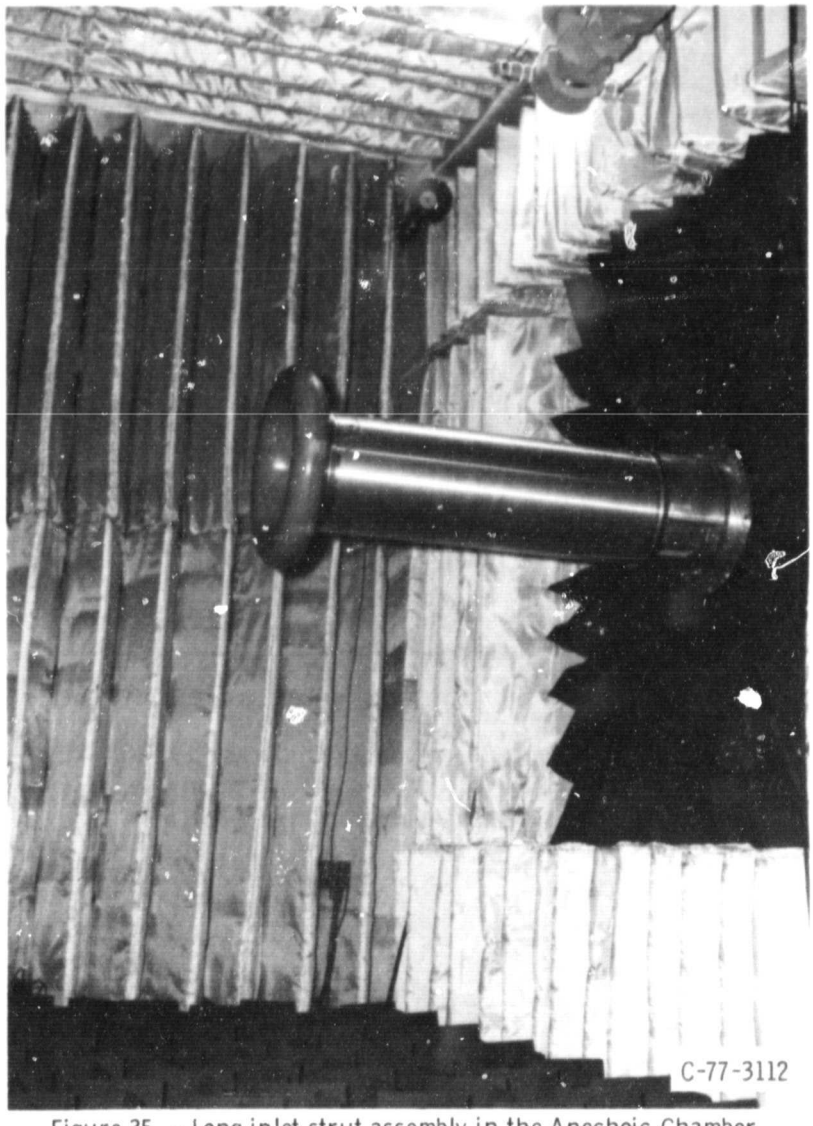

Figure 35. - Long inlet strut assembly in the Anechoic Chamber.

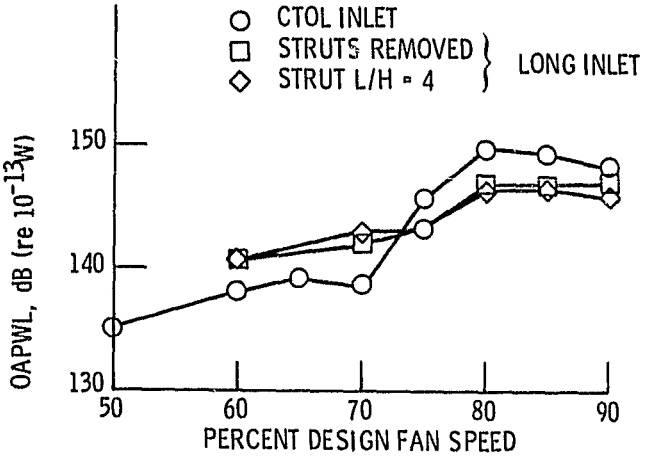

Figure 36. - Overall sound power level (0^0 - 90^0, 1 K - 20 KHz) as a function of fan speed showing effect of inlet configuration.

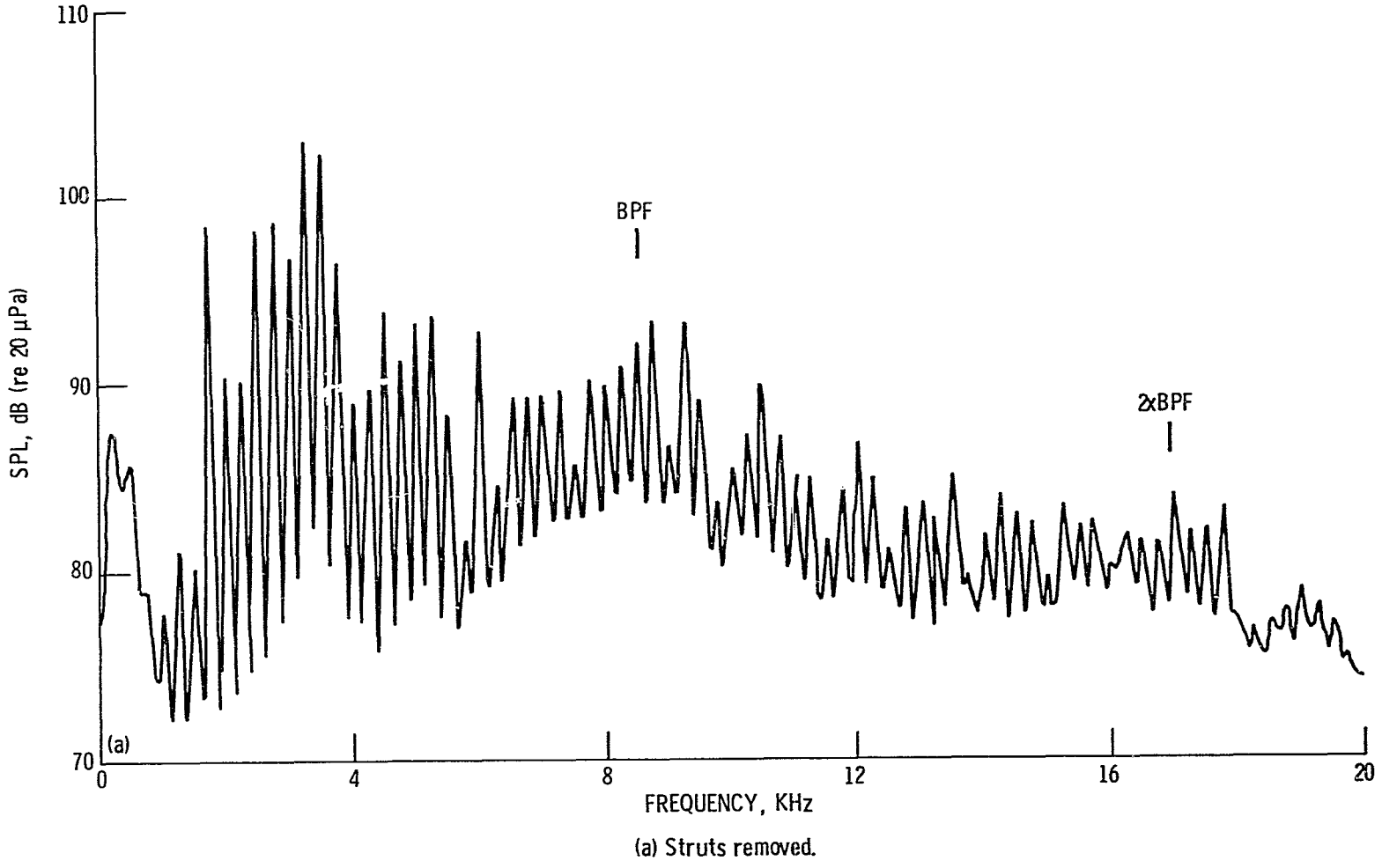

(a) Struts removed.

Figure 37. - SPL spectra at 70^0 for JT8D refan and long annular inlet duct (80% design speed).

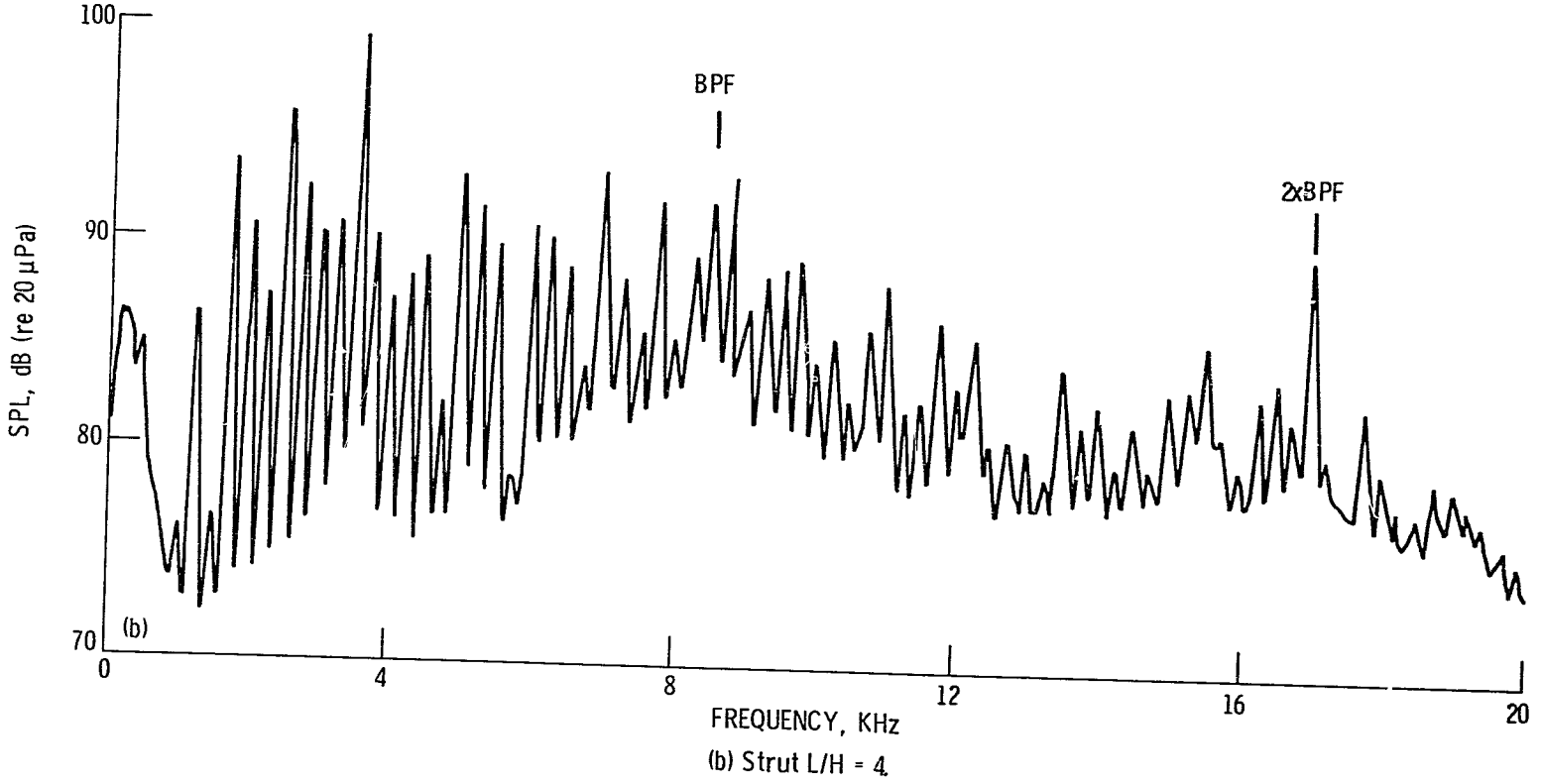

(b) Strut L/H = 4.

Figure 37. - Concluded.

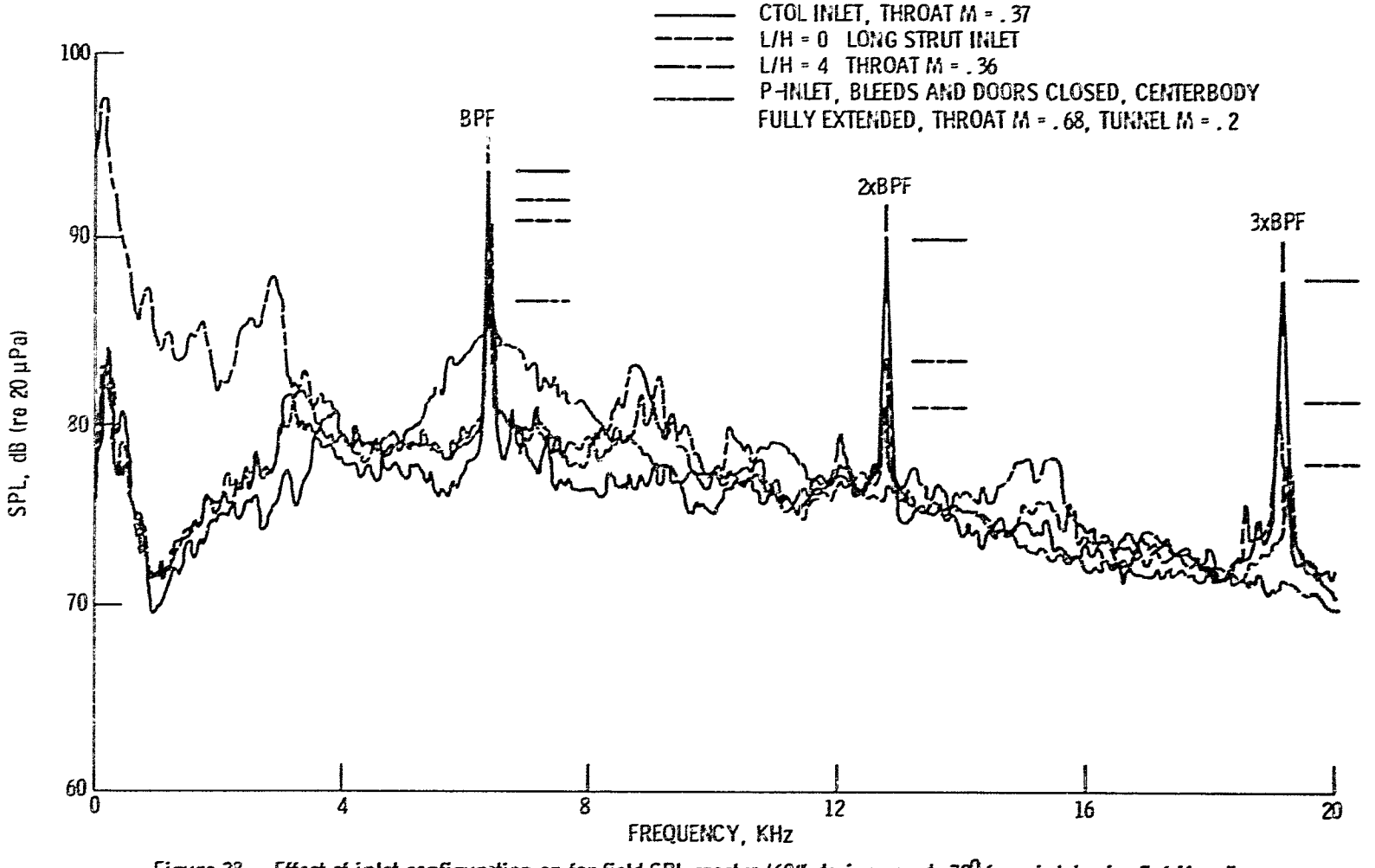

Figure 38. - Effect of inlet configuration on far field SPL spectra (60% design speed, 70° from inlet axis, 7.6 M radius).